Analytical and Bioanalytical Chemistry (2022) 414:7103–7122
https://doi.org/10.1007/s00216-022-04227-9

REVIEW

A colorimetric aptasensor based on gold nanoparticles for detection of microbial toxins: an alternative approach to conventional methods

Girma Salale Geleta[1]

Received: 11 June 2022 / Revised: 6 July 2022 / Accepted: 8 July 2022 / Published online: 29 July 2022

Abstract

Frequent contamination of foods with microbial toxins produced by microorganisms such as bacteria, fungi, and algae represents an increasing public health problem that requires the development of quick and easy tools to detect them at trace levels. Recently, it has been found that colorimetric detection methods may replace traditional methods in the field because of their ease of use, quick response, ease of manufacture, low cost, and naked-eye visibility. Therefore, it is suitable for fieldwork, especially for work in remote areas of the world. However, the development of colorimetric detection methods with low detection limits is a challenge that limits their wide applicability in the detection of food contaminants. To address these challenges, nanomaterial-based transduction systems are used to construct colorimetric biosensors. For example, gold nanoparticles (AuNPs) provide an excellent platform for the development of colorimetric biosensors because they offer the advantages of easy synthesis, biocompatibility, advanced surface functionality, and adjustable physicochemical properties. The selectivity of the colorimetric biosensor can be achieved by the combination of aptamers and gold nanoparticles, which provides an unprecedented opportunity to detect microbial toxins. Compared to antibodies, aptamers have significant advantages in the analysis of microbial toxins due to their smaller size, higher binding affinity, reproducible chemical synthesis and modification, stability, and specificity. Two colorimetric mechanisms for the detection of microbial toxins based on AuNPs have been described. First, sensors that use the localized surface plasmon resonance (LSPR) phenomenon of gold nanoparticles can exhibit very strong colors in the visible range because of changes caused by aggregation or disaggregation. Second, the detection mechanism of AuNPs is based on their enzyme mimetic properties and it is possible to construct a colorimetric biosensor based on the 3,3',5,5'-tetramethylbenzidine/Hydrogen peroxide, TMB/H_2O_2 reaction to detect microbial toxins. Therefore, this review summarizes the recent applications of AuNP-based colorimetric aptasensors for detecting microbial toxins, including bacterial toxins, fungal toxins, and algal toxins focusing on selectivity, sensitivity, and practicality. Finally, the most important current challenges in this field and future research opportunities are discussed.

Keywords Gold nanoparticles (AuNPs) · Colorimetric aptasensors · Microbial toxins · Aptamers

Introduction

Food contamination by microbial toxins produced by bacteria, fungi, and algae (such as fungal toxins, bacterial toxins, and algal toxins) is becoming a serious problem for human health [1]. The composition of microbial toxins varies from small organic molecules to macrobiomolecules (such as peptides and proteins) [2]. They are distributed all over the entire world and threatening the health and life of humans and livestock, and affecting domestic and international trade [3–5]. For example, bacterial toxins such as a staphylococcal toxin, clostridia botulinum toxin, Clostridium difficile toxin, Bacillus anthracis toxin, and Shiga toxins that cause various diseases are secreted in the food during growth [6]. Fungi can also produce small toxic hydrophobic metabolites called mycotoxins such as aflatoxins (AFs), ochratoxin (OTA), fumonisins (FB), zearalenone (ZEN), patulin (PAT), deoxynivalenol (DON), and trichothecenes. They are a major global health problem due to the fungal contamination of grains and peanuts and their persistence in food samples.

✉ Girma Salale Geleta
ggirma245@gmail.com

[1] Department of Chemistry, College of Natural Sciences, Salale University, P.O. Box 245, Oromia, Fiche, Ethiopia

It is estimated that more than 25% of the crops produced are contaminated with mycotoxins [7, 8], resulting in billions of dollars in losses each year [9]. In addition, cancer research institutes have reported that mycotoxins are considered carcinogenic, mutagenic, teratogenic, and tumorigenic due to their mode of action. Algal toxins such as microcystins (MCs), cylindrospermopsin (CYN), brevetoxin (BTX), okadaic acid (OA), anatoxins (ANTXs), and saxitoxins (STXs) are a secondary toxic metabolite caused by an algal bloom and also constitute a threat to the human health and the ecological environment as well. At very low concentrations and in their presence, some microbial toxins cause significant additive and/or synergistic toxicity or acute poisons [5]. Accurate analysis of microbial toxins in food ensures product quality, enforces regulatory requirements, and ensures compliance with national and international food standards to protect potential public health and safety threats. Therefore, it is important to develop methods of measuring microbial toxins in real samples from a variety of sources.

Several analytical methods have been developed for the detection of microbial toxins, including high-performance liquid chromatography (HPLC), high-performance liquid chromatography-tandem mass spectrometry (HPLC/MS/MS), and enzyme-linked immunosorbent assay (ELISA) [10, 11], and mouse bioassay (MBA) [12, 13]. HPLC-based methods are high reliability and accurate, but usually require expensive laboratory facilities and equipment, complex sample pre-treatment, and well-trained operators. These disadvantages severely limit the applicability of chromatographic analysis as a fast and easy-to-use on-site detection tool. Compared to chromatography, immunoassays use antibodies that are sensitive to pH and temperature, making them very susceptible to denaturation. In addition, the production of antibodies both in vitro and in vivo presents a challenge for the development of immunoassays as an alternative method to detect some toxins [14]. Therefore, the development of rapid, inexpensive, and sensitive analytical methods for monitoring microbial toxins remains highly desirable.

In the past decade, colorimetric biosensors have emerged as an alternative for microbial toxins detection because of their simplicity, low cost, high sensitivity, and specific detection, without the need for complex equipment. Various colorimetric sensing mechanisms, such as nanozyme catalysis, local surface plasmon resonance (LSPR), ligand-receptor binding, fluorescent on–off adjusting, and the color change of photonic crystals under-stimulation, are now well known, depending on the type of materials used to produce colorimetric sensors [15]. However, this review focuses on sensors that utilize the LSPR phenomenon of gold nanoparticles and its nanozyme catalysis to construct colorimetric sensors.

Colorimetric sensors based on localized surface plasmon resonance of gold nanoparticles (AuNPs)

Nanomaterials are often used for superior sensing applications in biosensors, to provide low detection limits and high sensitivity [16]. For example, due to their high extinction coefficient and size-dependent optical properties, AuNPs are widely used as colorimetric reporters to improve capture efficiency, signal amplification, and detection limit (DL) [17–23]. In particular, it is attracting more attention due to its strong light absorption in the visible region, mainly due to LSPR. LSPR is an optical phenomenon that results from the interaction of electromagnetic waves with the conduction of electrons in metals [24, 25]. Under the irradiation of light, the conduction electrons in the gold nanostructure are driven by the electric field to collectively oscillate locally at a resonant frequency relative to the lattice of positive ions (Fig. 1) [25–30]. Electromagnetic field decay length for localized surface plasmon is on the order of 6 nm (decay exponentially). The short field decay of the LSPR reduces the sensitivity of the solution to interference from refractive index fluctuations and increases the sensitivity to refractive index changes on the surface. The sensing capability of the LSPR absorption sensor can also be modified by tuning particle morphology, particle size, inter-particle interactions, particle composition, dielectric properties, and the local dielectric environment of the nanoparticle (refractive index) [31]. The principle of detection is based on the presence of any target analyte that can directly or indirectly trigger the aggregation redispersion of gold nanoparticles which results in a visible color change from red to blue or vice versa [26, 30–34].

AuNPs-based nanozymes colorimetric sensors

Recently, a new class of nanomaterials named nanozymes is a promising candidate for artificial biomimetic enzymes used to fabricate colorimetric sensors [35]. They were

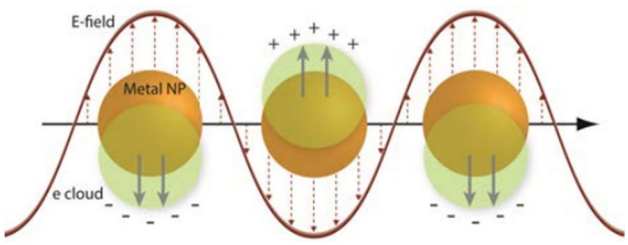

Fig. 1 Localized surface plasmon resonance (LSPR) scheme in which the free conduction electrons in metal nanoparticles are driven to oscillate due to strong coherence with incident light

developed to address the limitations of natural enzymes such as high costs in preparation and purification, low operational stability, difficulty in storage, and sensitivity of catalytic activity to specific working conditions (i.e., narrow substrate, temperature, and pH ranges) which often hampered the development and practical applications of colorimetric biosensors [36]. These gold nanoparticle-based nanozymes have shown several advantages over natural enzymes such as good conductivity, controlled synthesis at low cost, high stability against stringent conditions, and facile functionalization [37]. Studies conducted in recent years reported that gold nanoparticles have shown excellent enzyme mimetic activity similar to peroxidase, oxidase, catalase, superoxide dismutase, or reductase and therefore could be utilized for the fabrication of TMB/H_2O_2 reaction-based colorimetric sensors and biosensors [38]. The recognition mechanism of AuNPs is based on the oxidation of a variety of chromogenic substrates (e.g., 3,3′,5,5′-tetramethylbenzidine (TMB), 2,2′-azino-bis(3-ethylbenzthiazoline-6-sulfonic acid) (ABTS), 3,3′-diaminobenzidine (DAB), and o-phenylenediamine dihydrochloride (OPD)) in the presence of hydrogen peroxide (H_2O_2) and exhibiting a marked color change which is the basis of the colorimetric detection [39–42]. Nanozymes exhibit favorable catalytic activity, and their substrate selectivity is inadequate. For example, most peroxidases and oxidase mimics, nanozymes, catalyze not only the oxidation of TMB but also other substrates such as 2,2′-azino-bis(3-ethylbenzothiazoline-6-sulfonic acid)diammonium salt (ABTS) and OPD [43]. Improving the substrate specificity of nanozymes for the detection of food contaminants usually requires the integration of molecularly imprint polymers or biorecognition elements, such as nucleic acid probes, aptamers, and antibodies. For bacterial toxins, specifically designed peptides can be used to achieve specific detection by the enzymatic activity of several toxins, such as botulinum toxin [44, 45].

Among these, aptamers (single-stranded DNA or RNA oligonucleotides) are one of the most popular biorecognition elements due to their ability to selectively bind their target molecules, which helps improve the sensor specificity [46–50]. The molecular recognition of aptamers with the target compound is the result of intermolecular forces involving hydrogen bonds, stacking of aromatic rings, van der Waals forces, hydrophobic effect, and electrostatic interactions. As an alternative to conventional antibodies, aptamers have the distinct advantages of high stability, flexible chemical modification, high selectivity, low immunogenicity, biocompatibility, low cost, facile chemical synthesis, and high tolerance to pH and temperature [51–53]. Therefore, they have a great potential to be used to develop an AuNPs-based colorimetric aptasensor for the detection of microbial toxins in food and environment samples.

Aptamers, on the other hand, can be used as a new therapeutic tool to combat chronic infections, as they are also used to block the functionality of microbial toxins, apart from their use in aptasensors [54]. For example, it has been reported that it binds to and neutralizes *S. aureus* alpha toxin [55], *S. aureus* enterotoxin B (SEB) [56], staphylococcal enterotoxin A (SEA) [57], anthrax toxin [58], botulinum neurotoxins (BoNTs) [59], and aflatoxins B1 (AFB1) [60]. Due to their unique properties, aptamers are a simple and inexpensive treatment that has fewer side effects, is less toxic, and is less immunogenic than traditional antibiotics. Therefore, in addition to its use in aptasensors, it has the potential to be a powerful tool for the dissemination of new therapeutic factors with the ability to inhibit the function of microbial toxins.

This review, therefore, summarizes the recent application of AuNPs-based colorimetric aptasensor for the detection of microbial toxins, including bacterial toxins, fungal toxins, and algal toxins focusing particularly on selectivity, sensitivity, and practicality. To my knowledge, there are no systematic reviews that specifically focus on AuNPs-based on colorimetric aptasensor for detection of microbial toxins. To fill this gap, this systematic review summarizes the application of AuNPs for detecting microbial toxins using colorimetric aptasensors. Finally, it discusses the current major challenges and opportunities for future research in this field.

Detection of microbial toxins

Detection of bacterial toxins

Detection of botulinum neurotoxins

BoNT is produced by Clostridium botulinum and is classified into seven serotypes designated from A to G, each composed of a 100 kDa heavy chain (HC) and a 50 kDa light chain (LC). They are connected by disulfide bonds [11, 61, 62]. They cause botulism, a life-threatening neuroparalytic disease [63, 64]. Human botulism is caused by serotypes A, B, E, and sometimes F. Among them, type A is the most powerful and has the longest effect in vivo (up to 6 months) [65–67]. This toxin cleaves the soluble proteins of N-ethylmaleimide-sensitive factor attachment protein receptors (SNARE). For example, synaptosomal associated protein 25 (SNAP-25) is primarily cleaved by three serotypes A, C, and E at the residues 197–198, 198–199, and 180–181, respectively. Syntaxin is cleaved between residues 253 and 254 by serotype C. Synaptobrevin (VAMP) is cleaved between the amino acids 76–77, 59–60, 58–59, and 81–82 by serotypes B, D, F, and G [65, 68]. As a result, it blocks the release of acetylcholine from presynaptic nerve endings

at the neuromuscular junction of both the central and peripheral nervous systems, causing flaccid muscle paralysis [65].

Food poisoning, infant botulism, and wound botulism are the most common forms of this disease. For example, foodborne botulism is a form of poisoning mainly observed in humans, occurring when the bacteria Clostridium botulinum undergoes a growth phase that leads to the production of toxins in food before consumption. Ingestion of food contaminated with biologically active BoNTs can cause food poisoning and can cause respiratory paralysis, coma, and death in 70 kg humans after ingestion of only 70 µg [66]. These are potent bacterial toxins that contaminate the food supply and are likely to be exploited as bioterror agents. Currently, the most widely used detection method to monitor toxin activity is the mouse bioassay. This test is sensitive, but slow, expensive, has limited throughput, and poses ethical issues for the use of live animals. Therefore, it is important to develop a low-cost, easy-to-use, fast, and sensitive method for real-time monitoring of low-level BoNTs in foods.

For example, Chen et al. [67] have developed a sensitive colorimetric detection of BoNT activity using gold nanoparticles (Fig. 2). First, the SNAPtide, modified with biotin and cysteine in its two ends, would be cleaved into two short peptides by BoNT activity. The unreacted-cleaved peptides with biotin were removed by magnetic separation, leaving only the cysteine-terminated peptide. Next, AuNPs were added to bind with the cleaved peptides via the thiol group of cysteine. These peptide-functionalized AuNP aggregate and cause color changes upon addition of Cu^{2+}, enabling macroscopically identifiable colorimetric signals at a low concentration of 1 ng mL^{-1} (6.67 pmol L^{-1}). Due to spectral absorption, the detection limit is reached at 0.25 ng mL^{-1} (1.67 pmol L^{-1}, 3 σ/s). The main advantage of this methodology is the simplicity of the assays combined with the relatively high sensitivity. However, using AuNPs, Cu^{2+}, and modified magnetic micro-particles increases the cost. Also, like most assays, it has not been fully tested against different BoNT serotypes and different sample matrices. Based on a similar methodology, Halliwell and Gwenin [69] used AuNPs to detect BoNTs using the principle of utilizing the visible color change that occurs when colloidal gold is exposed to sodium chloride. The developed methodology uses the process of BoNT cleaving SNAP-25; nine amino acids are removed from the C-terminus of the protein. This shortening of SNAP-25 reduces the protective layer present around the AuNPs in the gold colloid which in turn increases their susceptibility to aggregation upon exposure to the sodium chloride. This assay is capable of detecting BoNT/A up to detection levels of 373 fg mL^{-1} by UV–vis spectroscopy on a semi-micro cuvette scale, and further developed a microscale assay for high throughput of samples, and were able to find the detection limit of 600 fg mL^{-1}.

Detection of Clostridium difficile toxin B

Clostridium difficile, an anaerobic, spore-forming, Gram-positive bacterium, is involved in nosocomial intestinal infections and can cause antibiotic-associated diarrhea and pseudomembranous colitis in humans and animals [70]. Most C. difficile strains produce two major toxins, i.e., TcdA and TcdB [71]. Toxin A (TcdA) is a deadly enterotoxin that can cause hemorrhage and fluid secretion. Toxin B (TcdB) is a very potent cytotoxin for many cultured cells [72]. Al-Saadi and co-workers have developed a prototype nano-gold assay to detect C. difficile toxin B directly and inexpensively. A total of 105 C. difficiles were clinically isolated, cultured, and DNA extracted. Subsequently, 17.3 µL of the extracted genomic DNA was restricted by the addition of 0.5 µL of the enzyme, 2 µL of buffer, and 0.2 µL of acetylated bovine serum albumin. It was then incubated at 37 °C for 1 h and inactivated at 65 °C for 20 min. The assay was performed as follows. The extracted DNA 22 µL (1.7 ng $µL^{-1}$) was placed in a sterile PCR tube. Next, 13 µL of hybridization buffer was added and mixed well (final concentrations of primer and NaCl after the addition of AuNP were 0.9 µmol L^{-1} and 0.04 mol L^{-1}, respectively)

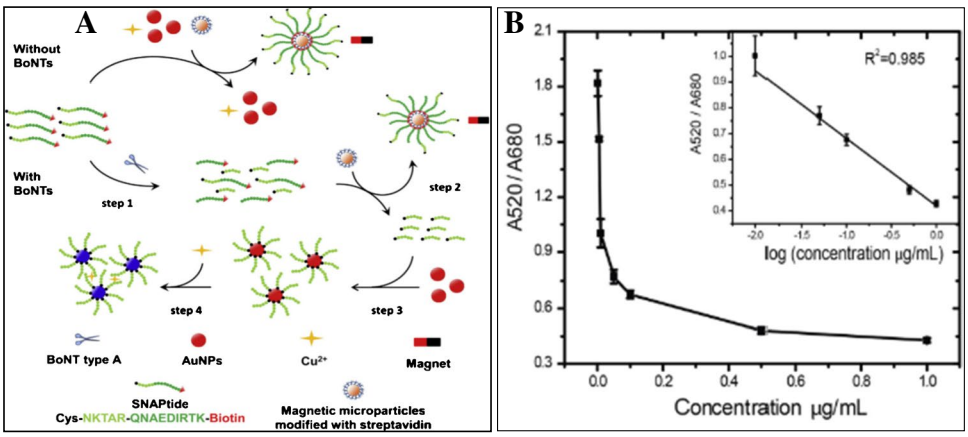

Fig. 2 **A** The working principle of the colorimetric detection of active botulinum neurotoxin (BoNT) using gold nanoparticles. **B** Absorbance ratio (A520/A680) of the AuNP solution (reproduced with permission from Shan et al. [67], Copyright 2016 Elsevier B.V.)

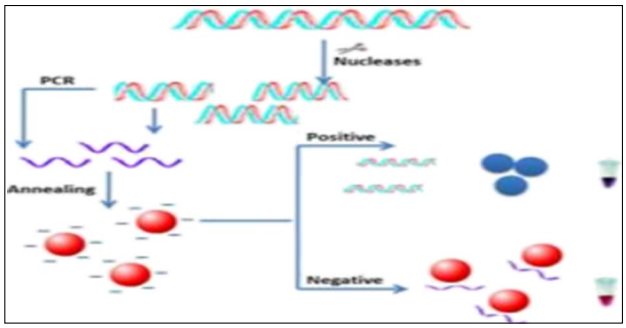

Fig. 3 Schematic diagram showing the principle of AuNPs-based colorimetric assay for C.difficiles and its toxin B. In positive samples, the primers were complementary to the DNA/RNA target and are not available in hybridization buffers containing NaCl to protect and stabilize AuNp, resulting in AuNP aggregation and blue formation. In contrast, if there is no target or non-specific DNA, the primer is released into the reaction mixture and binds with AuNP to prevent aggregation and the color does not change (reproduced with permission from Tahani et al. [73], Author(s) retain the Copyright 2017)

to obtain a final volume of 35 µL per PCR tube. The mixture was then heated to 95 °C for 30 s, annealed at 50 °C for 30 s, and then cooled to room temperature for 10 min. Next, 25 µL of colloidal AuNP was added to the mixture and the color was observed within 1 min. All C. difficile-positive specimens were further tested for toxin B according to a similar method for detecting C. diff DNA by AuNP, but with specific toxin B (Ted B) primers (5-CAC GCC TGG) (AGA ATC TAT ATT TGT AGA AA-3) (Fig. 3). It has been reported that the prototype's development is simple, sensitive, and fast, as evidenced by the color change from red to blue within a minute. They have also reported as the developed assay is cheaper than commercially available assays for clinically diagnose of C. difficiles toxin B, especially in developing countries [73].

Detection of staphylococcal enterotoxin B

Staphylococcal enterotoxins (SEs), an important group of heat-stable toxins produced by *S. aureus*, are associated with food-borne diseases resulting from the consumption of contaminated foods [74–78]. For example, SEB, with its high stability to heat and proteolytic activity, is a major cause of food poisoning and causes gastrointestinal symptoms such as vomiting, emesis nausea, and diarrhea. It is currently listed as a category B bio-weapon agent and anaphylactic shock with low levels of exposure (20–100 ng/person) [75]. In addition, SE is associated with the development of diseases such as atopic eczema, rheumatoid arthritis, and toxic shock syndrome. The lethal dose of SEB aerosol is 0.02 ng kg^{-1}, and it is estimated that it may induce an emetic response in humans as low as 0.4 ng kg^{-1} [79, 80]. Therefore, reliable and sensitive detection of SEB is important to avoid the potential risk to human health from foods contaminated with SEB.

Mondal and co-workers reported a simple, sensitive, and selective AuNPs-based colorimetric biosensor for the detection of SEB using SEB-binding aptamer as a recognition element. This assay is based on aptamer conformational change in the presence of SEB and a red-to-purple color change due to the phenomenon of salt-induced AuNP aggregation that can be monitored with the naked eye or with a UV–vis spectrometer. Results showed that the AuNPs could effectively differentiate the SEB-induced conformational change of the aptamer in the presence of a given high salt concentration. Linear responses were obtained with SEB concentrations ranging from 50 µg $mL^{-1}$to 0.5 ng mL^{-1}. This assay was highly specific for SEB compared to other related toxins. The detection limit (LOD) of SEB reached within a few minutes was visually improved from 50 to 0.5 ng mL^{-1} by spectroscopy [78]. Similarly, the detection of SEB by aptamer-based colorimetry using AuNPs as a probe was reported by the Liu group [79]. SEB could be detected at a concentration of 10 ng mL^{-1} by the AuNPs-based colorimetric method.

Zhou et al. reported colorimetric quantification of staphylococcal enterotoxin B by using gold nanoparticles with DNAzyme (Fig. 4) [80]. This assay is based on the growth of gold nanoparticles mediated by the hemin/G-quadruplex DNAzyme, which results in a red-to-blue color change in the presence of SEB. This method is enzyme-free and does not require labeling. The rate of AuNP formation is controlled by the hemin/G-quadruplex DNAzyme, which is the key to the signaling mechanism. In the presence of SEB, the aptamer target reaction regulated the amount of single-probe G-strands that form DNAzymes that can consume hydrogen peroxide. The AuNP growth process is affected by the resulting concentration of H_2O_2 and causes a color change. A wide linear range from 0.1 to 500 pg mL^{-1} was achieved and the detection limit was calculated to be 1 pg mL^{-1}.

Detection of fungal toxins

Mycotoxins

Of the 300 mycotoxins identified and reported, the most important are AF, OTA, fumonisin, patulin, ZEN, trichothecene, DON, and T2 toxin [81]. The principle of mycotoxin detection using a colorimetric sensor is based on the protection of AuNP from salt-induced aggregation by aptamers due to the strong van der Waals interaction between DNA bases and gold. This electrostatic affinity induces aptamer adsorption that stabilizes dispersed nanoparticles. During recognition of mycotoxins, aptamers desorb from the surface of AuNP and preferentially form a complex with the target. Subsequently, under the action of the electrolyte or cationic

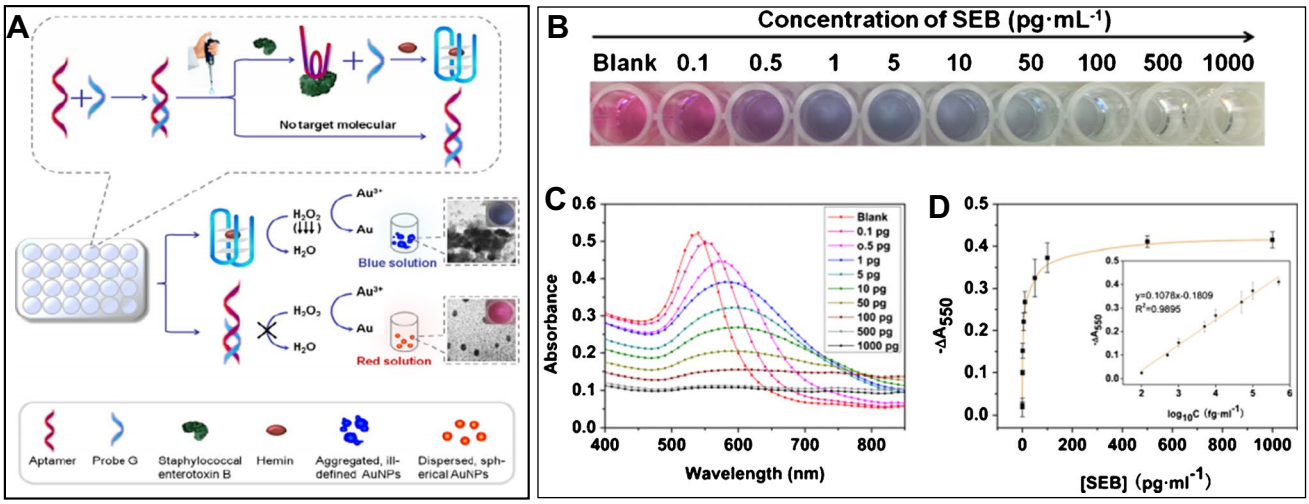

Fig. 4 **A** Schematic diagram of colorimetric analysis of SEB detection based on DNAzyme led to the growth of AuNPs. **B** Photograph of AuNPs grown for macroscopic SEB detection. **C** Corresponding plasmon absorption spectra of different SEB concentrations. **D** The linear range between the decrease in absorbance at 550 nm and the log concentration of SEB (reproduced with permission from Dandan et al. [80], Copyright 2016 Springer-Verlag Wien)

polymer, stable gold aggregates are formed, which leads to a change in the color of the solution. This aptasensing strategy has been widely reported (label-free AuNP-based aptasensors) for the rapid detection of mycotoxins such as aflatoxins B1, B2, AFM1, ochratoxin A, and zearalenone.

Detection of aflatoxins

Aflatoxin is a mycotoxin produced by molds *Aspergillus flavus* and *Aspergillus parasiticus*, present in a wide range of food products [82–85]. AFs play an important role in developing countries; they have acute toxicity and can lead to cancer, immunologic suppression, and nutritional interference [85, 86]. The most common AF are aflatoxins B_1, B_2, G_1, G_2, M_1, and M_2. Among them, AFB1 is usually predominant in amount (75%) and constitutes the most toxic, which is listed as group I carcinogen by the International Agency for Research in Cancer [87–92]. It is with this concern that most countries have established exposure limits for AFB1 in China and the USA, the maximum permissible level of AFB1 is 20 μg kg^{-1} (parts-per-billion (ppb)) in corns and groundnuts [84]. To prevent food safety scares, and avoid subsequent economic losses, various methods have been developed for the detection of AFB1, like HPLC/fluorescence [90], ultra-high-performance liquid chromatography-tandem mass spectrometry [91], HPLC-MS/MS [92], and immunochromatography [93] such as commercially available lateral flow strip assays [94], ELISA [95], and electrochemical immune analysis [96]. Although these approaches are highly sensitive, simpler, and cost-effective methods are still desirable. Alternatively, colorimetric biosensors are considered a promising sensor platform for detecting mycotoxins because of their cost-effectiveness, ease of use, and macroscopic readability [1].

Recently, Kasoju et al. reported an aflatoxin B1 aptasensor that can detect aflatoxin B1 using a specific aptamer–gold nanoparticles called AFB1–Apt–AuNPs nanoconjugates on a microfluidic paper-based analytical device (μPAD). The Apt–AuNPs nanoconjugates were adsorbed to paper by physical adsorption and AFB1 flowed over the μPAD [97]. In the absence of aflatoxin B1, aptamers were adsorbed on the AuNPs surface by physical adsorption, increasing the stability of the AuNPs in the presence of NaCl and the color of AuNPs remained red. In presence of aflatoxin B1, the aptamer bound to AuNPs is replaced, forming a complex with aflatoxin B1 leaving AuNPs to react with NaCl causing aggregation (change in color from wine red to blue). Microfluidic devices showed an excellent response to the detection of aflatoxin B1 in the range of 1 pmol L^{-1} to 1 μmol L^{-1} with a detection limit of up to 10 nmol L^{-1} in spiked samples. Using a similar principle, Kasoju and coworkers developed colorimetric detection of aflatoxin M1 (AFM1) in milk samples using a μPAD [98]. The detection mechanism of aflatoxin M1 detection is based on aptamer-modified AuNPs. AuNPs citrate capped showed aggregation in the presence of NaCl. AuNPs bound to particular aptamers remained dispersed in the presence of NaCl. Aggregation is caused by the addition of AFM1, which displaced specific aptamers and causes aggregation of AuNPs in the presence of NaCl. A paper microfluidic device in which milk samples containing AFM1 are moved by capillarity and quickly turn blue color due to aggregation of specific aptamers with AFM1. On the other hand, in the control (without AFM1 aptamer), no aggregation was observed. The analytical linear

range is 1.00 µmol L^{-1} to 1.00 pmol L^{-1}, and the detection limit is 3 pmol L^{-1} and 10 nmol L^{-1} in standard buffer and spiked milk samples, respectively, was observed by naked eyes, similar to the results obtained with AFB1.

Luan et al. have developed a label-free aptasensor for detecting AFB1 using the unmodified AuNPs and AFB1 binding DNA aptamer. Aptamers were adsorbed on the AuNP surface based on electrostatic interactions. The electrostatic repulsive force improves the stability of AuNPs against NaCl-induced aggregation. Upon addition of the target, the AFB1-aptamer complex was formed, the surface of AuNPs separated, and salt-induced aggregation of AuNPs occurred. These events changed the wine-red color to blue-purple, which could be easily observed with the naked eye or measured with a UV-vis spectrometer. The linear response and detection limit of this system were determined to be 0.025–100 ng mL^{-1} and 0.025 ng mL^{-1}, respectively. The method presented was fast, sensitive, simple, and inexpensive [99]. Chen et al. [100] developed an AuNPs-based colorimetric aptasensor using an enzyme-free catalytic DNA circuit for amplified detection of aflatoxin B1. The calculated LOD was 2 pmol L^{-1}, with a wide linear range from 10 pmol L^{-1} to 1 µmol L^{-1}. Recently, Zhu et al. [101] fabricated a colorimetric biosensor for simultaneous ochratoxin A and aflatoxins B1 detection in agricultural products. The detection ranges for AFB1 and OTA were found to be 5–250 ng mL^{-1} and 0.5–80 ng mL^{-1}, respectively.

A label-free colorimetric aptasensor for rapid detection of AFB1 was developed using a specific aptamer, cationic perylene probe (CPP), and unmodified citrate–stabilized AuNPs (Fig. 5) [102]. In the absence of AFB1, free specific aptamer forms a complex structure with the CPP, resulting in the solution remaining red without aggregation of AuNPs. On the other hand, in the presence of AFB1, the aptamer competes to interact with AFB1 and CPP. In particular, aptamers are highly specific for AFB1 and are CPP-free in solution. Supplementation with AuNP stabilized with unmodified citrate turns the color blue as a result of CPP-induced aggregation of AuNP. The color change of AuNP is due to localized surface plasmon resonance absorption associated with nanoparticle size, shape, and aggregation. This phenomenon can be measured by colorimetric detection, and the analytical linear range was found to be 1–10 ng mL^{-1} by a spectrophotometer and 1–6 ng mL^{-1} by a homemade LED-LDR colorimeter, respectively. Using a detector spectrophotometer and a homemade colorimeter, they found that the detection limits were 0.36 and 0.18 ng mL^{-1}, respectively. In a real application, the proposed method should be combined with the affinity column as sample preparation.

Another aflatoxin, aflatoxins B2 (AFB2), is a highly toxic, teratogenic, mutagenic, and carcinogenic metabolite produced by fungi of the genus Aspergillus, mainly *Aspergillus flavus*, *Aspergillus parasiticus*, and *Aspergillus nomius* [81]. Studies have shown that aflatoxin species exhibit immunosuppressive effects as a result of the inhibition of DNA, RNA, and protein synthesis by a variety of mechanisms.

Luan et al. used gold nanoparticles to create a colorimetric detection of AFB2 (Fig. 6) [103]. In the absence of aflatoxin B2, the aptamer's random coil structure stabilizes the surface of AuNPs and shows a red color under high NaCl conditions. In the presence of aflatoxin B2, the formation of aflatoxin B2-aptamer conjugate destabilizes AuNPs from NaCl-induced aggregation and changes the color of the dispersion. This method was characterized by a linear dynamic range of 0.025 to 10 ng mL^{-1}, and a detection limit of 25 pg mL^{-1}. This is lower than the MRL (maximum residue level) of edible foods set by China and the European Commission. In addition, this method was able to detect AFB2 with high selectivity when AFB1 was present as an interfering substance. This AFB2 detection method

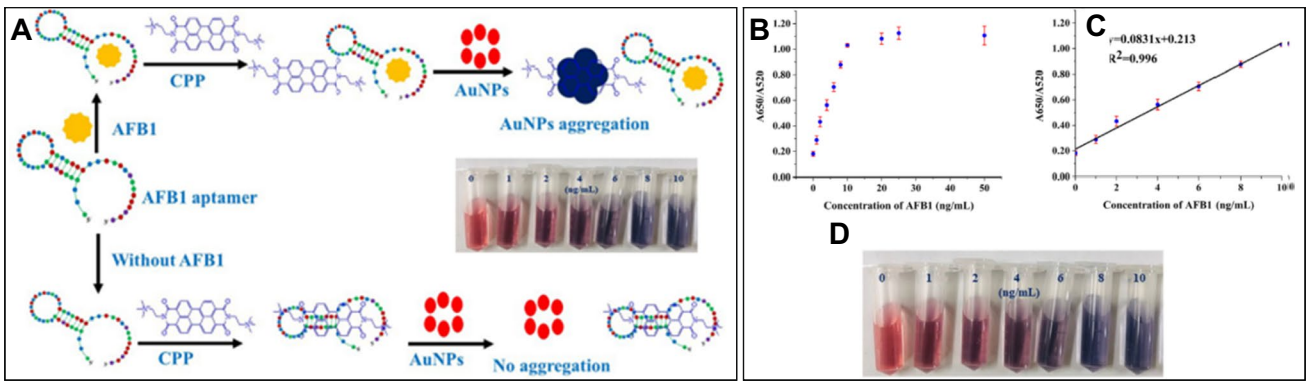

Fig. 5 **A** Schematic diagram of AFB1 detection with a label-free colorimetric aptamer using specific aptamers, CPPs, and AuNP based on localized surface plasmon resonance absorption. **B** Ratios of AFB1 to A650/A520 at various concentrations were detected by spectrophotometers. **C** Linear calibration curve plots, and **D** images of AFB1 at various concentrations (reproduced with permission from Jamras et al. [102], Copyright 2020 Elsevier B.V.)

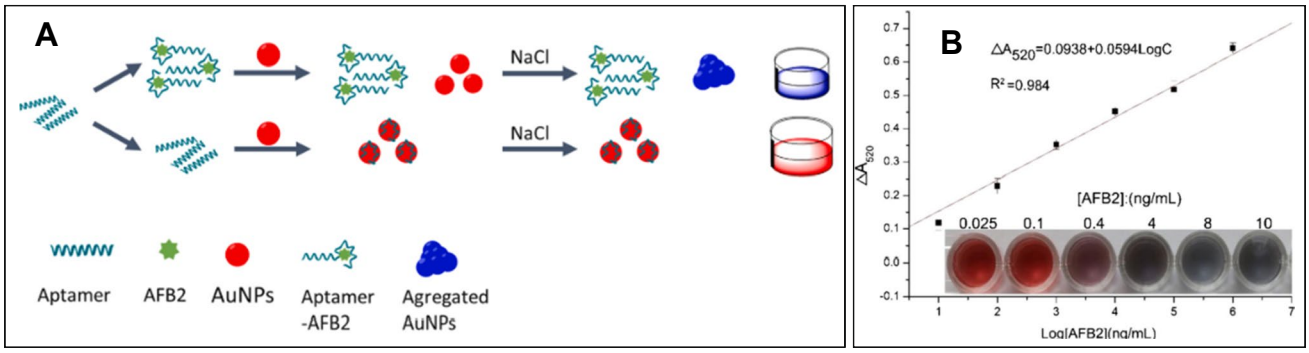

Fig. 6 **A** Schematic diagram showing an aflatoxin sensor for detecting AFB2 with AuNP. **B** Typical calibration curve of AFB2 obtained with an aptamer-based biosensor (insertion diagram: corresponding photographic image of AuNP solution) (reproduced with permission from Luan et al. [103], Copyright 2014 Springer-Verlag Wien)

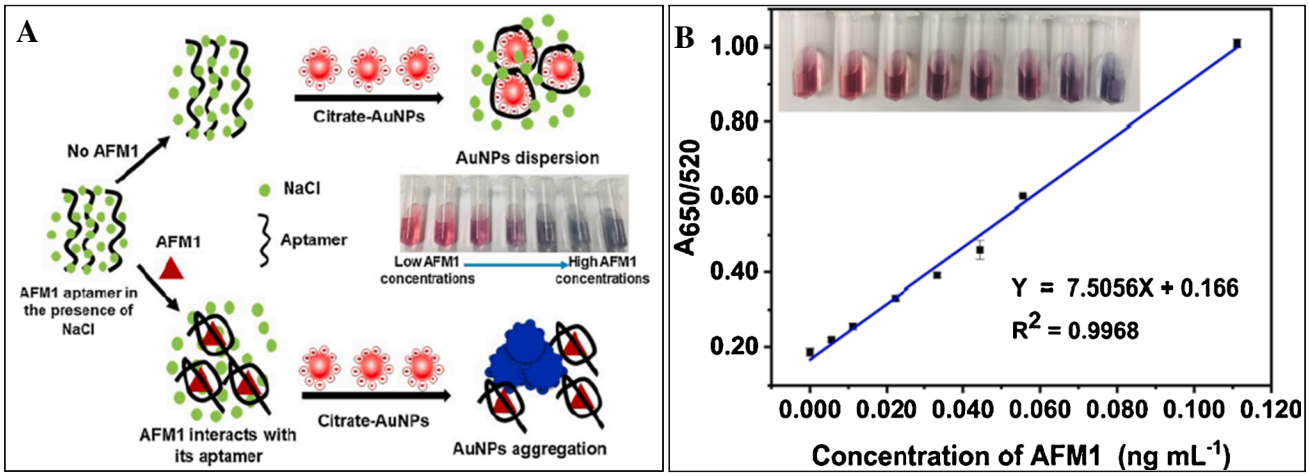

Fig. 7 **A** Visualized mechanism of the colorimetric aptasensor for AFM1 detection. **B** Linear calibration curve plots (inset shows the color of the corresponded standard solutions) (reproduced with permission from Kasoju et al. [104], Copyright 2021 Elsevier Inc.)

has several advantages over other analytical methods such as high sensitivity, high stability, short analysis time, and cost-effectiveness in food and agricultural products.

A label-free colorimetric aptasensor for measuring AFM1 based on LSPR and aggregation of AuNPs has been reported (Fig. 7) [104]. It is based on the competitive interactions of aptamer with AuNPs or AFM1 in the presence of sodium chloride. Aptamers interact selectively with AFM1 and cannot prevent sodium chloride-induced aggregation of AuNPs. The color change of the solution caused by the shift of the LSPR peak aggregated AuNPs was measured by the colorimetric method. They found that the detection limit was 0.002 ng mL^{-1}. In addition, it reported that the recovery rate was found to be over 80% and the RSD was less than 10%.

An optical aptasensor has been developed for AFM1 detection based on salt-induced aggregation and target-induced protection of gold nanoparticles. For this assay, streptavidin-coated silica nanoparticles (SNPs) (dsDNA) modified with aptamer/were prepared. With the addition of AFM1, the AFM1 aptamer attached to AFM1 and the CS aptamer displaced from aptamer/AFM1-modified SNPs, and the free CS adsorped on the surface of AuNPs and protect AuNPs against salt-induced aggregation. On the other hand, in the absence of AFM1, SNPs (dsDNA) modified with aptamer/CS is stable and CS cannot bind to AuNP, resulting in salt-induced aggregation of AuNP and the sample turning purple. The proposed aptasensor can detect AFM1 with a linear dynamic range of 300–75,000 ng L^{-1}, with a detection limit of 30 ng L^{-1}. This detection method was also effectively applied to the detection of AFM1 in the milk samples [105].

The colorimetric approach has attracted sensing methods due to its simplicity and the observation of color changes in the sample with the naked eye [106]. A colorimetric aptasensor has been introduced for sensitive detection of AFM1 based on the catalytic activity of CRISPR-Cas12a, rolling

circle amplification (RCA), and AuNPs. In the presence of AFM1, the CRISPR-Cas12a is inactivated and the addition of T4 DNA ligase and phi29 DNA polymerase forms a large single-stranded DNA (ssDNA) structure on the surface of AuNP. After adding nitrophenol, the color of the sample remains yellow. However, due to CRISPR-Cas12a activation and primer digestion, no large DNA structure is observed on the surface of AuNP in the absence of a target. Therefore, the color of the sample changes to colorless. The results showed that the biosensor showed high selectivity for AFM1 and the approach reached the detection limit of only 0.05 ng L^{-1}. In addition, the spiked milk sample AFM1 can be identified with high sensitivity. Overall, this approach is extremely sensitive and does not require complex equipment. Therefore, it still holds a promising potential for the detection of other mycotoxins in real samples by simply replacing the applied sequences.

Detection of ochratoxin

OTA, a toxic secondary metabolite, is primarily derived from species of the genera Aspergillus and Penicillium [107–111]. In addition, it is found in large quantities in various types of foods and beverages such as wheat, corn, coffee, cocoa, beer, wine, and dried fruit [112, 113]. OTA has strong hepatotoxicity, neurotoxicity, immunotoxicity, renal toxicity, teratogenicity, carcinogenicity, and mutagenic effects [114–117] and is classified as a group 2B carcinogen. Moreover, OTAs are also highly chemically and thermally stable, very difficult to remove once they enter the food chain, and are expected to seriously endanger people's health [118]. OTA has also been reported to affect protein synthesis and apoptosis, immunosuppression, immune system depletion, suppression of antibody responses, altered immune cell activity, and inhibition/activation of enzymes involved in the regulation of cytokine production [119, 120]. However, traditional assays for detecting OTA are expensive and complex. Alternatively, colorimetric aptasensors using unmodified gold nanoparticles have received a great deal of attention due to their low cost, simplicity, and practicality, and have been developed for a variety of purposes in recent years [115].

Recently, a colorimetric aptamer based on the enzyme-induced aggregation of AuNPs was developed by combining the highly sensitive enzyme-mediated aggregation of AuNPs with the efficient binding ability of an aptamer toward

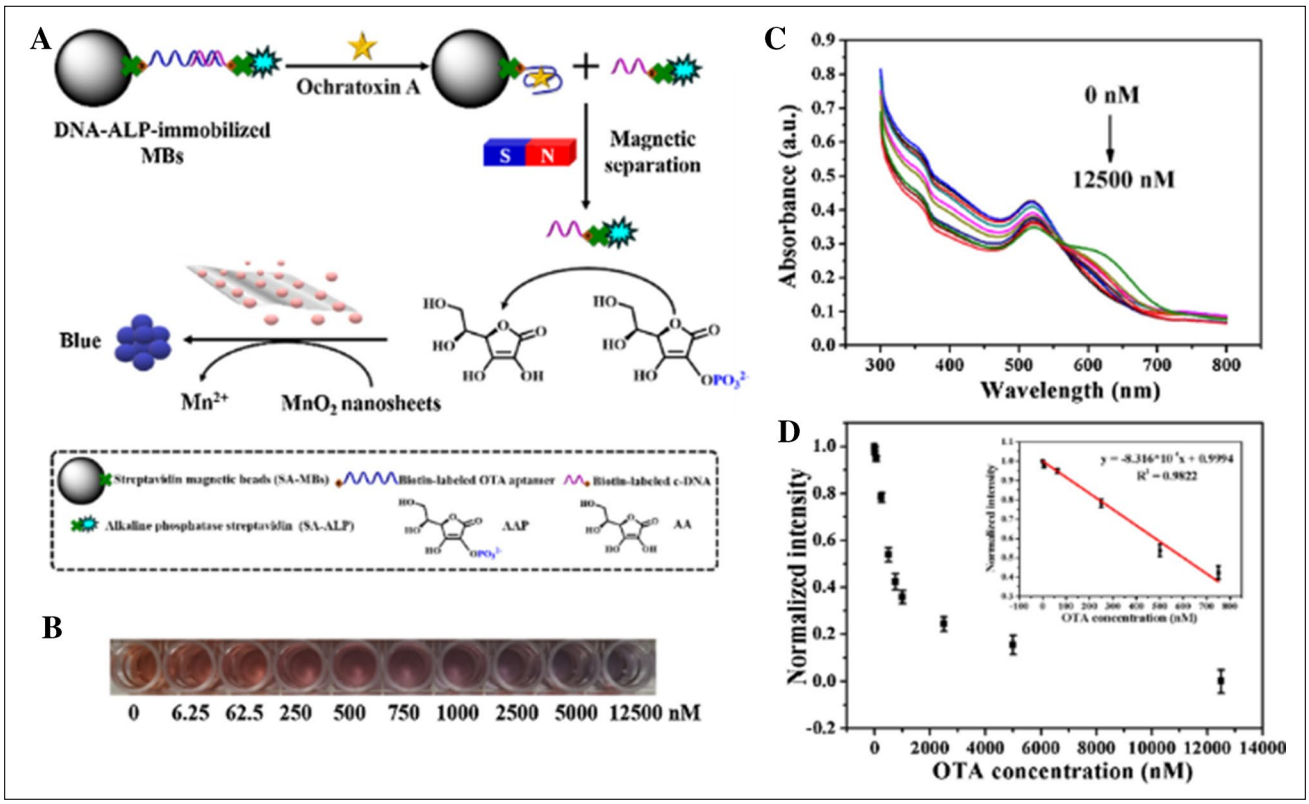

Fig. 8 **A** Schematic of the mechanism of colorimetric aptasensor based on an enzyme-induced aggregation of AuNPs for OTA detection. **B** Visual photo of semi-quantitative determination of OTA. **C** UV–vis absorption spectra in the presence of different OTA concentrations. **D** The relationship between the normalized absorption intensity at 520 nm versus different OTA concentrations [1]. (Reproduced with permission from Yue et al. [1], Copyright 2019 Elsevier B.V.)

OTA (Fig. 8) [1]. This colorimetric method was developed to detect OTA indirectly via alkaline phosphatase (ALP) activity. Briefly, aptamer-modified magnetic beads (MBs) are bound to DNA-bound ALP by hybridization. After OTA detection, magnetic separation was able to collect the amount of the released enzyme. ALP then hydrolyzes ascorbic acid 2-phosphate (AAP) to ascorbic acid (AA), which mediates the reduction of MnO_2 nanosheets to Mn^{2+}. These metal cations allow AuNPs to aggregate, resulting in color changes in the sensor system. The dynamic range was 6.25 to 750 nmol L^{-1}, and an improved LOD of 2 ng·mL^{-1} was recorded. This colorimetric method was applied to the matrix of grape juice and red wine matrix with sufficient recovery.

On the other hand, a label-free aptamer-based assay has been developed for sensitive and specific detection of OTA using a cationic polymer and AuNPs [119]. OTA aptamers have been used as recognition elements for OTA colorimetric detection based on AuNPs aggregation by the cationic polymer. By spectroscopic quantitative analysis, colorimetric analysis was able to detect OTA up to 0.009 ng mL^{-1} with high selectivity in the presence of other interfering toxins [119]. Xiao et al. have demonstrated a colorimetric detection method based on the disassembly of AuNP dimers to detect OTA. The system featured low detection of 0.05 nmol L^{-1}, with a dynamic range of 0.2 to 250 nmol L^{-1} [120]. The proposed sensor was used to detect OTA in red wine. The OTA concentration measured by this method was consistent with the results obtained with a commercially available ELISA kit.

Interestingly, Liu et al. reported gold nanoparticle-aptamer-based LSPR detection of ochratoxin A in the extended detection range by calibration curves obtained at low and high OTA concentrations [115]. Yang and co-workers have developed a colorimetric detection method for OTA using unmodified AuNPs as an indicator and its aptamer as a specific recognition element. OTA's aptamers are easily adsorbed onto the surface of AuNPs, improving the stability of AuNPs against salt aggregation. However, in the presence of OTA, the conformation of the OTA aptamer changed from a random coil structure to a G-quadruplex structure thus losing the ability to protect AuNPs. Upon the addition of salt, electrostatic repulsion between AuNPs was screened, resulting in the aggregation of AuNPs. The detection could be realized by monitoring the color change of the AuNPs even with naked eyes. The linear range of the colorimetric aptasensor covered a large variety of OTA concentrations from 20 to 625 nmol L^{-1} and the detection limit of 20 nmol L^{-1} was obtained [121].

Multicolor detection of OTA has also been reported by etching AuNRs (diameter ~ 14 nm) mediated by G-quadruplex (AG4-OTA)-hemin DNAzyme and exonuclease I [110]. TMB^{2+}, a product of peroxidase-like activity in acidic solutions, can etch AuNR by oxidizing Au (0) to Au (I). Changes in AuNR's optical properties due to changes in inter-particle distance and the number of hydrogen bonds are described as a key sensing strategy. The linear response range of 10 to 200 nmol L^{-1} OTA and LOD was found to be as low as 30 nmol L^{-1} by visual observation and 10 nmol L^{-1} by spectrophotometric. Selectivity for OTA was tested using the interfering mycotoxins AFB1, ZEN, and OTB. This method was successfully used to determine the OTA of a spiked beer sample.

Recently, Tain et al. reported the multi-colorimetric detection of ochratoxin A by enzymatic metallization of gold nanorods and structural switching aptamers using a similar approach (Fig. 9) [122]. DNA ALP immobilized magnetic beads using streptavidin and biotin-labeled OTA aptamers. In the presence of OTA, aptamers bind to OTA to form G-quadruplexes and release ALP-tagged complementary DNA (cDNA-ALP). After magnetic separation, cDNA-ALP catalyzed the decomposition of ascorbic acid-2-phosphate into ascorbic acid reduced Ag^{+} and formed an Ag shell on the surface of AuNR. This caused a blue shift in the vertical local surface plasmon resonance peak of AuNR, resulting in a macroscopic change visible to the naked eye. Linear response range 12.5 to 20,000 nmol L^{-1} OTA with LOD 9.0 nM was reported. This method demonstrates the potential for on-site visual semi-quantitative detection of mycotoxins in foods.

Fe_3O_4NP (Au @ Fe_3O_4) doped with AuNPs was synthesized in one step by a simple solvothermal method. The peroxidase-like activity of Au @ Fe_3O_4NP was effectively enhanced by the synergistic effect of Fe_3O_4NP and AuNP. Based on this, an efficient colorimetric aptasensor has been developed that takes advantage of Au @ Fe_3O_4NP's unique dual function as a signal indicator and magnetic separator. First, an amino-modified aptamer specific for OTA was surface-attached to the surface of amino-terminal glass beads using glutaraldehyde as a linker. Next, amino-modified capture DNA (cDNA) was labeled with amino-functionalized Au @ Fe_3O_4NP, and an aptamer was constructed by hybridization reaction between cDNA and aptamer. On the other hand, when added, the OTA-aptamer complex was formed and Au @ Fe_3O_4NP bound to cDNA was released into the bulk solution. By simple magnetic separation, the collected Au @ Fe_3O_4NP can produce a blue solution in the presence of 3,3′,5,5′-tetramethylbenzidine, and H_2O_2. When the reaction is stopped by adding H^{+} ions, the blue product can turn into a yellow product with higher absorbance. This colorimetric aptasensor can detect only 30 pg mL^{-1} OTA with high specificity. They have reported that this colorimetric aptasensor utilizes for the first time the peroxidase-like activity of nanomaterials for OTA detection and provides an effective route for routine food safety quality control [123].

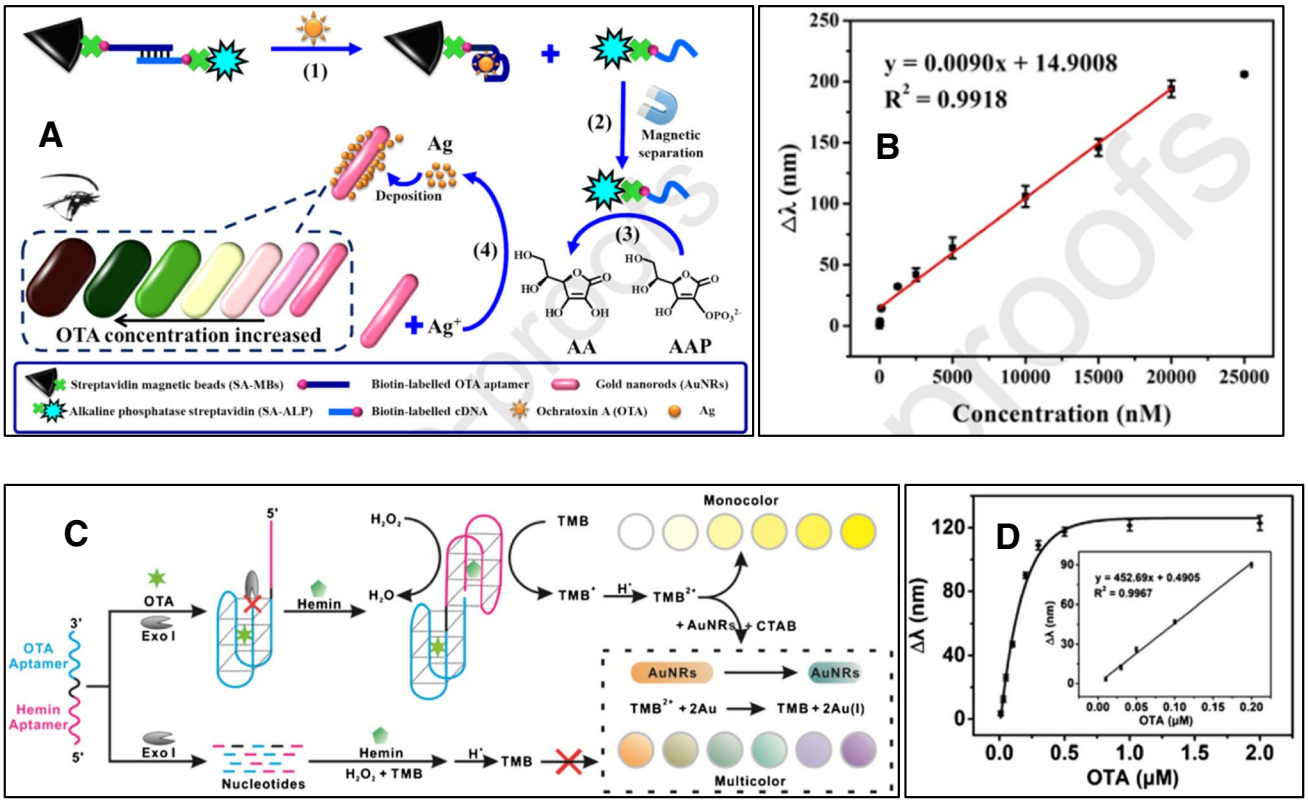

Fig. 9 **A** Working principle of the multi-colorimetric detection of OTA based on the structural switching of aptamer and the enzyme-induced deposition of AuNRs. **B** Multicolor colorimetric detection of OTA via structure-switching aptamer and enzyme-induced metallization of gold nanorods. **C** The schematic illustration of the principle of exonuclease-assisted multicolor OTA detection. **D** Calibration curve for detecting the different concentrations of OTA. (Reproduced with permission from Xinhui et al. [118], Copyright 2018 Springer-Verlag GmbH; Fengyu Tiana et al. [122], Copyright 2020 Elsevier Ltd.)

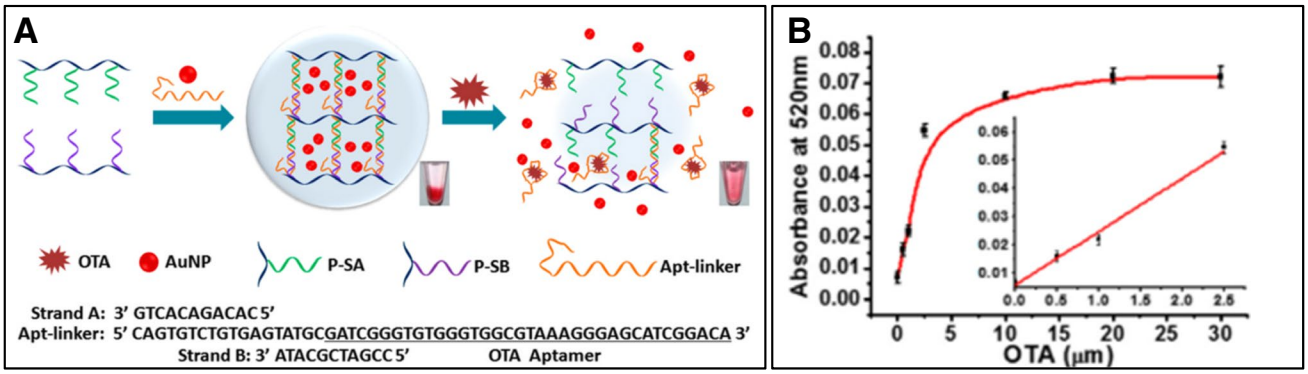

Fig. 10 **A** The working principle of DNA hydrogel encapsulated in AuNP for visual detection of OTA. Incorporation of OTA causes the hydrogel to disintegrate and release AuNP, resulting in a supernatant changing from colorless to red. This can be observed with the naked eye. **B** The standard working curve was obtained by monitoring the absorbance of the supernatant at 520 nm (reproduced with permission from Rudi et al. [124], Copyright 2015 American Chemical Society)

Targeted aptamer-crosslinked hydrogels have been designed and synthesized for portable and visual quantitative detection of OTA in foods and beverages by Liu et al. (Fig. 10) [124]. The hydrogel network is formed by hybridization between a designed DNA strand containing an OTA aptamer and two complementary DNA strands grafted onto a linear polyacrylamide strand. Upon introduction of OTA, aptamers bind to OTA and cause hydrogel dissociation. It then releases preloaded AuNPs that are visible to the naked eye. To enable sensitive visual and quantitative detection,

Au @ Pt core–shell nanoparticles (Au @ PtNPs) were encapsulated in hydrogels to produce a quantitative display on a volume bar graph chip (V-chip). In the V-chip, Au @ PtNP catalyzes the oxidation of H_2O_2 to produce O_2. This guides the color bar to move to a concentration-dependent distance for visual quantitative reading. In addition, OTA immunoaffinity column (IAC) was introduced, which concentrates OTA from beer, to improve the detection limit of complex real samples. After enrichment, V-chip can detect only 1.27 nmol L^{-1} (0.51 ppb), which meets the European Commission's test requirements (2.0 ppb). The integration of target-responsive hydrogels with IAC's portable enrichment, signal amplification, and quantitative readout with a simple microfluidic device provides a new method for portable detection of the food safety hazard toxin OTA.

Detection of ZEN

ZEN is a type of resorcylic acid lactone, a secondary metabolite produced by several Fusarium species. A mycotoxin that poses a food safety threat and is found in most grains such as rice, wheat, corn, barley, oat, sorghum, sesame, hay, and corn silage [125]. Chronic exposure to ZEN can cause serious side effects such as neurotoxicity, carcinogenicity, and immunotoxicity. In addition, ZEN as mycoestrogen can impair reproduction and affect the endocrine system [86]. Therefore, innovations in the design of analytical techniques for detecting ZEN are very important.

Recently, zearalenone was determined using Au nanoparticles modified with a specific aptamer (Fig. 11C) [47]. In the absence of a target, the aptamers are involved in a hybridization reaction with a complementary sequence on

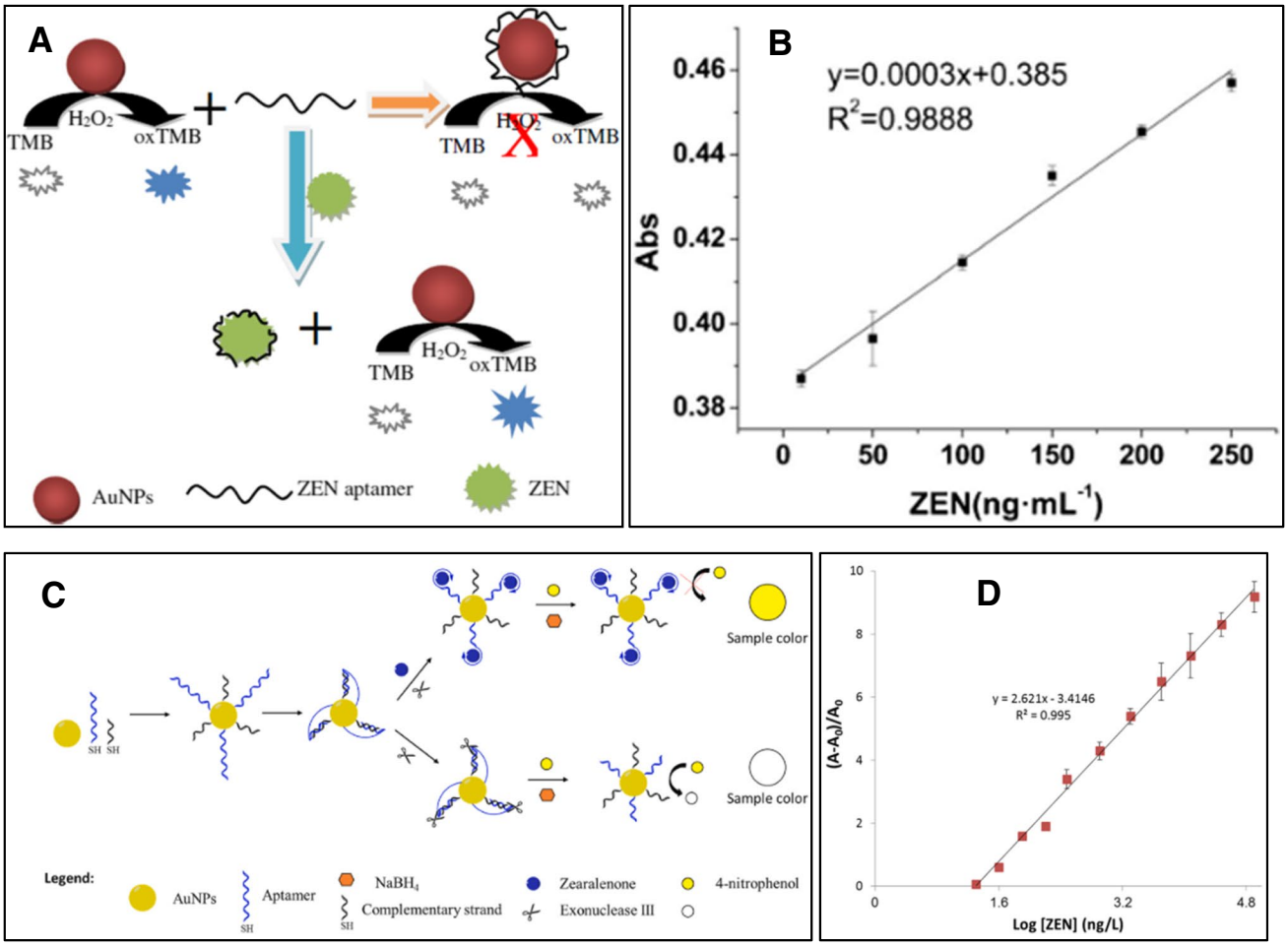

Fig. 11 **A** Schematic illustration of the principle of AuNP nanozyme assay for ZEN detection. **B** Linear correlation between the concentration of ZEN and absorbance of samples at 630 nm under the optimal reaction condition. **C** Schematic representation of the colorimetric aptasensor for the detection of ZEN, based on the Exo III-assisted aptamer walker and the catalytic reaction of AuNPs. **D** Calibration curve of the ZEN aptasensor. A_0 and A are the absorbances at 400 nm before and after the addition of various concentrations of ZEN, respectively [44, 71, 117] (reproduced with permission from Shumin et al. [47], Copyright 2018 Springer-Verlag GmbH; Seyed et al. [126], Copyright 2018 American Chemical Society)

the surface of Au nanoparticles. In the presence of zearalenone, double-stranded DNA dissociates. The color change is associated with the catalytic oxidation of aminophenol on the exposed golden surface. Treatment of the system with exonuclease increases the signal by digesting the hybridized DNA and recycling the analyte bound within the surface layer. Low ZEN requirements and signal amplification are some of the distinct advantages of the proposed aptasensor. The presented aptasensor was able to detect ZEN with a wide linear dynamic range of 20−80 000 ng L^{-1}, with a detection limit of 10 ng L^{-1}. The aptasensor has been applied to human serum, with a detection limit of 40 ng L^{-1}, spiked serum sample recovery of 95–103%, and relative standard deviations (RSDs) of 7.1% or less.

Sun and co-workers have developed an aptamer-based colorimetric analysis for measuring ZEN [126]. It is based on the inhibition of AuNP's peroxidase-mimetic activity by ZEN aptamers. In the absence of ZEN, ZEN aptamers are absorbed on the surface of AuNPs by electrostatic interaction, and the shield on the surface of AuNP inhibits the peroxidase-like activity of AuNPs to oxidize TMB. However, in the presence of ZEN, aptamers bind to ZEN due to their high specific affinity and are unable to adsorb AuNPs due to structure change, promoting the recovery of AuNP's peroxidase-like activity and changing the colorless TMB into blue oxTMB. The color change can be observed with naked eyes. The linear range of this aptasensor has been determined to be 10–250 ng mL^{-1} and provides a LOD of 10 ng mL^{-1}. The specificity of the assay was validated by examining the effect of potential interferents. The recoveries ranged from 92 to 110%, and the standard deviation varied from 2.4 to 6.4%, demonstrating the good accuracy of this sensing system.

Detection of algal toxins

Detection of microcystins

Algal toxins can cause neurotoxicity, hepatotoxicity, and cytotoxicity in humans through the consumption of contaminated water and food [127–129]. Microcystin-LR (MC-LR), which contains leucine (L) and arginine (R), is a known group of algal toxins produced by cyanobacteria that are harmful to animals and human health [130, 131]. MCs are cyclic polypeptides composed of five constant amino acids and two different L-amino acids, forming a family of congeners that have different toxicities [132–135]. Acute poisoning with MC-LR causes skin irritation, diarrhea, and liver damage and poses a serious threat to water supply around the world. WHO has established guidelines for microcystin-leucine-arginine (MC-LR) in drinking water to be less than 1 μg L^{-1}, including both free and intracellular toxins [136–138]. Several analytical techniques have been developed to determine MC-LR including immunoassays, HPLC, liquid chromatography-mass spectrometry (LC–MS), and whole-cell bioassays. However, these methods require complex sample preparation, expensive equipment, highly specialized skills, and a lot of time [137]. Therefore, research on new methods for detecting MC-LR at low concentrations is becoming an increasingly important topic.

Recently, Li and co-workers [138] have developed a sensitive colorimetric aptasensor for detecting MC-LR in real water samples (Fig. 12). In this case, aptamer-modified surface AuNP prevents electrostatically induced aggregation of AuNP to high salinity. Without aptamer modification, elevated salt concentrations bring about aggregation which manifests as a change in the color of the solution. When MC-LR was added, the MC-LR-aptamer complexes caused the aptamer to break away from the surface of AuNPs, leading to the aggregation of AuNPs, and the color converted from red to blue. No change in color is observed when the system is challenged with competing analytes, demonstrating sensor selectivity. The detection limit was reached at 0.37 nmol L^{-1}.

On the other hand, Wang and co-workers demonstrated MC-LR colorimetric detection based on the disassembly of AuNP dimers bound by aptamers. In the absence of the target molecules, the aptamers acted as linkers, causing the asymmetrically modified AuNP to form a dimer, making the solution appear blue. On the other hand, if a target molecule is present, the aptamer undergoes a structural change process when it binds to the target molecule. This decomposed the AuNP dimer and changed the color of the solution to red. The proposed biosensor LOD was reported to be 0.05 nmol L^{-1} (Fig. 12) [139]. Recently, Gue and co-workers have shown that forming AuNP dimers, as opposed to larger-scale aggregates, results in an improvement of not only the sensitivity but also the dynamic range and long-term stability of such colorimetric-based biosensors. In addition, they showed that a significant improvement in LOD is achievable because the distance between particles is minimized when a Y-shaped DNA double chain is formed during dimer formation [33].

A sensitive and easy approach for colorimetric quantification of MC-LR in fish tissue is obtained by AuNPs and a truncated aptamer Apt-910–2, which was obtained by mutation and rational truncation from the previously selected 60-mer one. The binding affinity and specificity of the 23-mer Apt-910–2 for MC-LR have been improved as compared to the selected 60-mer one. The linear operating ranges of aptasensor are determined to be 10 to 150 ng mL^{-1}

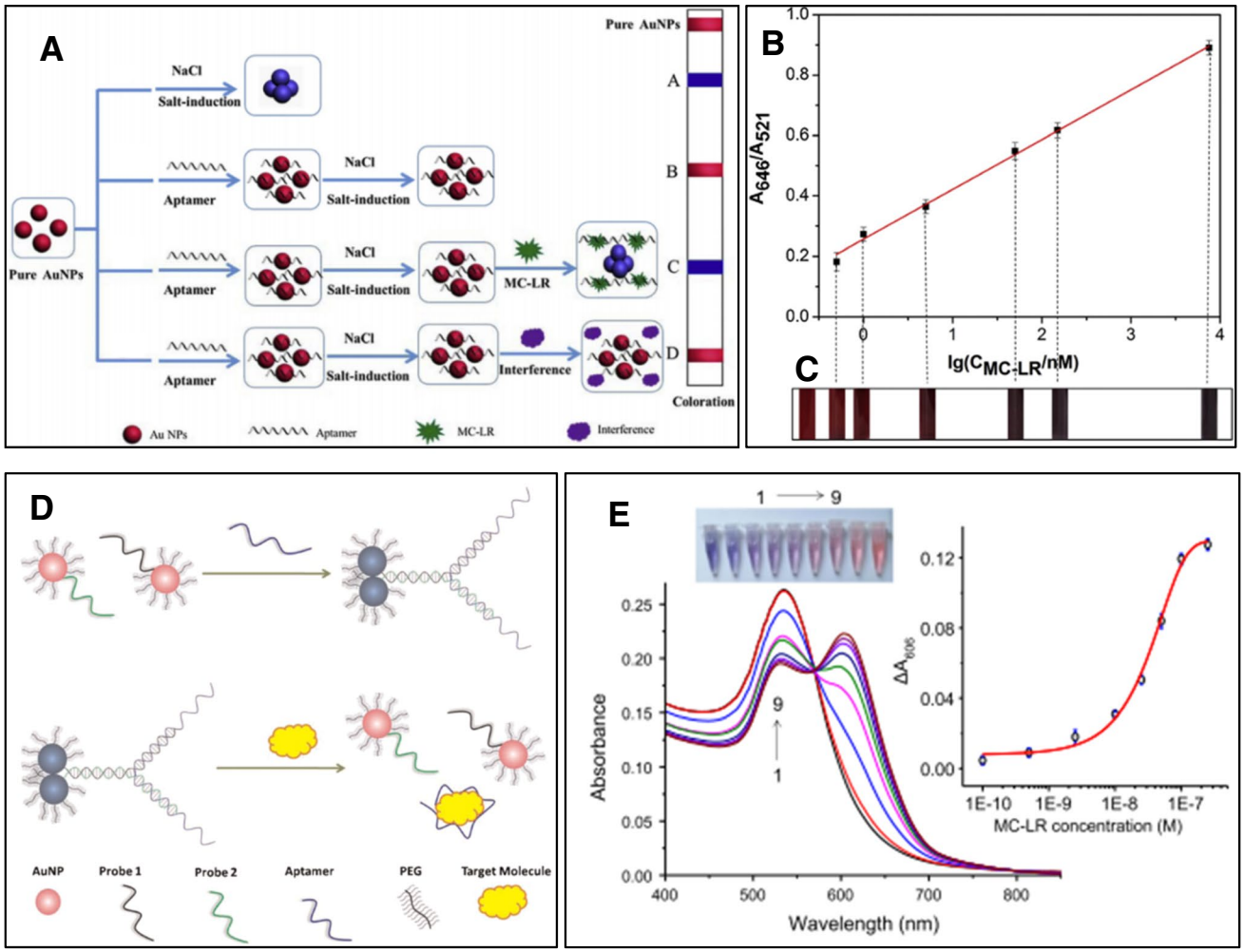

Fig. 12 **A** Schematic illustration for the colorimetric sensor and the mechanism for the analytic determination of MC-LR. **B** The linear calibration curve of A646/A521 versus the logarithm of MC-LR concentrations from 0.5 nmol L^{-1} to 7.5 µmol L^{-1}. **C** The corresponding color changes of AuNPs under different concentrations of MC-LR (0.5 nmol L^{-1} to 7.5 µmol L^{-1}). **D** Schematic diagrams representing the formation and disassembly of AuNP dimers. **E** Extinction spectra of the sensors in response to different concentrations of MC-LR of sample numbers 1 to 9 were 0, 0.1, 0.5, 2.5, 10, 25, 50, 100, and 250 nmol L^{-1}, respectively. The inset located at the top right shows the calibration curve for MC-LR detection (reproduced with permission from Xiuyan et al. [138]; Fangfang et al. [139], Copyright 2015 Elsevier B.V.)

and the LOD is found to be 0.38 ng mL^{-1}. Applicability was confirmed using spiked fish tissue samples with recovery rates ranging from 75.18 to 87.72% and with the visual LOD of 10 µg kg^{-1} in fish tissue judged by the naked eye [140].

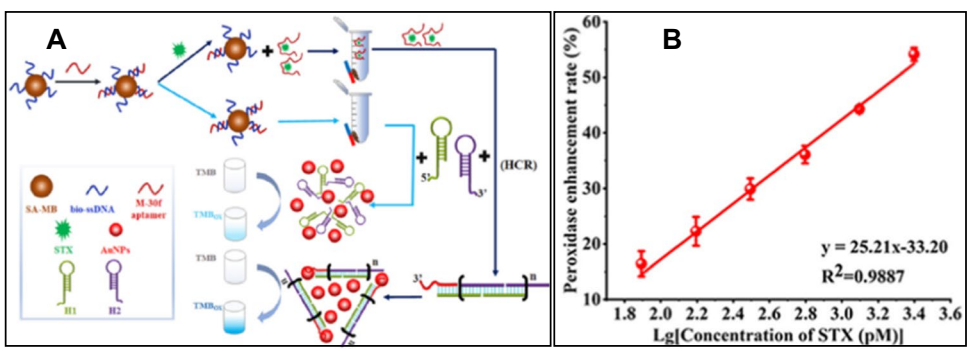

Fig. 13 **A** Schematic illustration of the competitive colorimetric aptasensor transduced by hybridization chain reaction-facilitated catalysis of AuNPs nanozyme for highly sensitive detection of saxitoxin. **B** Linear detection curve of the aptasensor (reproduced with permission from Yinglin et al. [143], Copyright 2021 Elsevier B.V.)

Table 1 Colorimetric aptasensors based on AuNPs for the detection of microbial toxins: linear range and limits of detection (LODs)

Microbial toxins	Mechanism of colorimetric detection	Linear range	Limit of detection (LOD)	References
Bacterial toxins				
BONT/A	SPR	10−0.001 ng mL^{-1}	0.25 ng mL^{-1}	[67]
	SPR	250–1500 fg mL^{-1} 600–2000 fg mL^{-1}	373 fg mL^{-1} (cuvette) 600 fg mL^{-1} (96-well plate)	[69]
SEB	SPR	50,000−0.5 ng mL^{-1}	0.5 ng mL^{-1}	[78]
	SPR	10−50 ng mL^{-1}	10 ng mL^{-1}	[79]
	SPR	0.0001−0.5 ng mL^{-1}	0.001 ng mL^{-1}	[80]
Fungal toxins				
AFB1	SPR	0.001−1000 nmol L^{-1}	10 nmol L^{-1}	[97]
	SPR	0.025−100 ng mL^{-1}	0.025 ng mL^{-1}	[99]
	SPR	0.1−1000 nmol L^{-1}	0.002 nmol L^{-1}	[100]
	SPR	1–10 ng mL^{-1} by a spectrophotometer and 1–6 ng mL^{-1} by a homemade LED-LDR colorimeter	0.36 ng L^{-1} 0.18 ng mL^{-1} (homemade colorimetry)	[102]
AFB2	SPR	0.025−10 ng mL^{-1}	0.025 ng mL^{-1}	[103]
OTA	Nanozymes-based probe	6.25 to 750 nM	5.0 nmol L^{-1}	[1]
	SPR	20−625 nmol L^{-1}	20 nmol L^{-1}	[121]
	Nanozymes-based probe	10–200 nmol L^{-1} OTA	30 nmol L^{-1} by visual observation 10 nmol L^{-1} by spectrophotometry	[110]
	SPR	0.05 to 50 ng mol L^{-1}	0.009 ng mL^{-1}	[119]
	Nanozymes-based probe	12.5–20,000 nmol L^{-1}	9.0 nmol L^{-1}	[122]
	SPR	0.2−250 nmol L^{-1}	0.05 nmol L^{-1}	[120]
AFM1	SPR	0.005−0.100 ng mL^{-1}	0.002 ng mL^{-1}	[104]
	SPR	1 µmol L^{-1} to 1 pmol L^{-1}	3 pmol L^{-1} in standard buffer 10 nmol L^{-1} spiked milk samples	[98]
	SPR	300–75,000 ng L^{-1}	30 ng L^{-1}	[105]
	Nanozymes-based probe	0.2–300 ng L^{-1}	0.05 ng L^{-1}	[106]
ZEN	Nanozymes-based probe	20−80 000 ng L^{-1}	10 ng L^{-1}	[47]
	Nanozymes-based probe	10–250 ng mL^{-1}	10 ng mL^{-1}	[126]
Algal toxins				
MC-LR	SPR	0.5–7500 nmol L^{-1}	0.37 nmol L^{-1}	[138]
	SPR	0.1–250 nmol L^{-1}	0.05 nmol L^{-1}	[139]
Saxitoxin	Nanozymes-based probe	78.13 to 2500 pmol L^{-1}	42.46 pmol L^{-1}	[143]
	SPR	10 fmol L^{-1} to 0.1 mmol L^{-1}	10 fmol L^{-1}	[142]

Abbreviations of microbial toxins: Ochratoxin A (OTA), aflatoxin B1 (AFB1), aflatoxin M1 (AFM1), botulinum neurotoxin (BoNT/A), staphylococcal enterotoxin B (SEB), zearalenone (ZEN)

Detection of saxitoxin

STX is a shellfish paralytic poison (SPT) that accumulates in shellfish tissues throughout the food chain and can cause symptoms of toxicity in various system organs when humans ingest toxin-contaminated seafood. This toxin is easily absorbed from the gastrointestinal tract and is not destroyed by human digestive enzymes. It is stable even at high temperatures and in acidic solutions and poses a great danger to human health [141]. Currently, the main methods for detecting saxitoxin are HPLC, MBA, LC–MS/MS, and ELISA. However, these traditional methods have several limitations, including the need for technicians, expensive equipment, time consumption, and animal ethics issues. Therefore, there is an urgent need to develop a fast, selective, and sensitive on-site STX detection method for seafood safety and quality monitoring.

For example, Qiang et al. [142] have prepared AuNPs and aptamer (AuNPs-aptamer) biosensors for specific and quantitative detection of STX. AuNPs were protected from salt-induced aggregation by specific aptamers. However, in the presence of STX, the aptamer reacts specifically with STX resulting in the color change of the AuNP solution. The

detection limit was reported to be 10 fmol L^{-1} (3 fg mL^{-1}), and a good linear relationship was found in the range of 10 fmol L^{-1} to 0.1 mmol L^{-1}. The STX detection time is 30 min and is used for specific detection of STX in seawater.

Zhao et al. [143] reported a competitive colorimetric aptasensor transduced by hybridization chain reaction-promoting catalysis of AuNPs nanozyme for sensitive detection of saxitoxin (Fig. 13). The anti-STX aptamer hybridized to the complementary strand on the magnetic beads and was competitively bound by STX. The supernatant containing the aptamer that binds to STX was obtained by magnetic separation. This triggers a hybridization chain reaction (HCR) to produce variable length, sticky, rigid double-stranded DNAs (dsDNA). These HCR-dsDNA were found to be able to significantly enhance the peroxidase-like catalytic capacity of AuNPs nanozyme for TMB. The concentration of STX was responded to in a "turn on" mode, based on its enhanced color conversion. Aptasensor achieves high sensitivity with a LOD of only 42.46 pM. In addition, analysis of STX from real samples achieved a wide linear detection range of 78.13 to 2500 pM, and analysis of STX from shellfish samples showed good selectivity and good recovery of 106.2 to 113.5% was obtained. This strategy can be used to develop robust aptasensors for easy and sensitive detection of other small molecules and toxins. Table 1 summarizes the linear ranges and limit of detections (LODs) for some important mycotoxins,algal toxins,and bacterial toxins described in this review.

Conclusions and outlook

This review summarizes recent applications of colorimetric aptasensors based on localized surface plasmon resonance of AuNPs for the detection of microbial toxins. Gold nanoparticle-based colorimetry aptasensors are inexpensive, easy to handle, can be analyzed in the field with the naked eye, and have no prerequisite for modern equipment. However, there are still some limitations and challenges that need to be addressed. First, the interference in analyzing real-world samples remains a challenge limiting the wide range of applications of AuNP-based colorimetric assays. Therefore, when analyzing a real sample, sample preparation techniques should be used to reduce matrix interference. Second, it requires improved selectivity, sensitivity, and narrow dynamic range compared to other analytical techniques such as chemiluminescence and fluorescence. To improve the selectivity, highly specific aptamers with strong affinities for microbial toxins should be incorporated into the AuNP nanoprobe. On the other hand, it is necessary to improve the sensitivity of colorimetric measurement by using signal amplification to detect microbial toxins. For example, AuNP-based detection strategies have been combined with the reduction of silver (I) to provide signal amplification leading to a LOD improvement by several orders of magnitude. In addition, increasing the size of the AuNPs and decreasing the density of the receptor groups on the surface of each AuNPs will increase sensitivity. Third, large-scale synthesis methods of AuNPs with uniform performance are lacking for their wide range of applications. Despite the challenges mentioned above, colorimetric aptasensors based on localized surface plasmon resonance of AuNPs are particularly promising for the development of colorimetric aptasensor for onsite detection of microbial toxins, especially in underdeveloped areas without advanced equipment. On the other hand, the peroxidase-like activity of gold nanoparticles was recently utilized to build a colorimetric detection platform for microbial toxins. AuNPs-based nanozymes have outstanding advantages over traditional biocatalytic approaches, such as ease of synthesis, low cost, tunable activity, long shelf life, and high environmental stability, but several challenges remain to be overcome. One of the biggest challenges is the low selectivity of the nanozymes compared to natural enzymes. To improve the substrate specificity of nanozymes for enzyme activity, there are several studies based on binding strategies that induce the presence of substrate binding sites to biomolecules, imprint polymers, or aptamers. Another potential strategy to improve both activity and substrate specificity is to use assemblies of nanozymes or complex structures containing nanozymes and natural enzymes. Despite some success with AuNPs-based colorimetric nanozyme aptasensors for the detection of microbial toxins, research in this area is still in its infancy. Therefore, AuNPs-based nanozyme colorimetric aptasensors are expected to make important contributions in the field of biosensing for measuring microbial toxins in the future.

Acknowledgements The author gratefully acknowledges the Department of Chemistry, Salale University.

Declarations

Conflict of interest The author declares no competing interests.

References

1. He Y, Tian F, Zhou J, Zhao Q, Fu R, Jiao B. Colorimetric aptasensor for ochratoxin A detection based on enzyme-induced gold nanoparticle aggregation. J Hazard Mater. 2020;388:121758.
2. Gupta R, Raza N, Bhardwaj SK, Vikrant K, Kim KH, Bhardwaj N. Advances in nanomaterial-based electrochemical biosensors for the detection of microbial toxins, pathogenic bacteria in food matrices. J Hazard Mater. 2021;401:123379.

3. Li Y, Liu D, Zhu C, Shen X, Liu Y, You T. Sensitivity programmable ratiometric electrochemical aptasensor based on signal engineering for the detection of aflatoxin B1 in peanut. J Hazard Mater. 2020;387:122001.
4. World Health Organization IA for R on C. IARC monographs on the evaluation of carcinogenic risks to humans. Some traditional herbal medicines, some mycotoxins, naphthalene, and styrene. IARC Press. 2002;82:1–556.
5. Smith MC, Madec S, Coton E, Hymery N. Natural Co-occurrence of mycotoxins in foods and feeds and their in vitro combined toxicological effects. Toxins. 2016;8:94.
6. He Y, Wen C, Guo Z, Huang Y. Noble metal nanomaterial-based aptasensors for microbial toxin detection. J Food Drug Anal. 2020;28:508–20.
7. Bhat R, Rai RV, Karim AA. Mycotoxins in food and feed: present status and future concerns. Compr Rev Food Sci Food Saf. 2010;9.
8. Enyiukwu DN, Awurum AN, Nwaneri JA. Mycotoxins in stored agricultural products: implications to food safety and health and prospects of plant-derived pesticides as a novel approach to their management. Greener J Microbiol Anti M. 2014;2:032–48.
9. Firew TM, Birhan AA, Kassahun T, Chengrong N, Gang W, Yang L. Mycotoxins in Ethiopia: a review on prevalence, economic and health impacts. Toxins. 2020;12:648.
10. Asensio L, Gonzalez I, Garcia T, Martin R. Determination of food authenticity by Enzyme-Linked Immunosorbent Assay (ELISA). Food Control. 2008;19:1–8.
11. Sharma SK, Ferreira JL, Eblen BS, Whiting RC. Detection of type A, B, E, and F Clostridium botulinum neurotoxins in foods by using an amplified enzyme-linked immunosorbent assay with digoxigenin-labeled antibodies. Appl Environ Microbiol. 2006;72:1231–8.
12. Pellett S, Tepp WH, Johnson EA. Critical analysis of neuronal cells and the mouse bioassay for detection of botulinum neurotoxins. Toxins. 2019;11(12):1–23.
13. Singh AK, Stanker LH, Sharma SK. Botulinum neurotoxin: Where are we with detection technologies? Crit Rev Microbiol. 2013;39(1):43–56.
14. Olasunkanmi OO, Richard AM. Aptamer utility in sensor platforms for the detection of toxins and heavy metals. J Toxins. 2017;4(1):1–12.
15. Liu B, Zhuang J, Wei G. Recent advances in the design of colorimetric sensors for environmental monitoring. Environ Sci Nano. 2020;7(8):2195–213.
16. Zahra QUA, Luo Z, Ali R, Khan MI, Li F, Qiu B. Advances in gold nanoparticles-based colorimetric aptasensors for the detection of antibiotics: An overview of the past decade. Nanomaterials. 2021;11(4):840.
17. Quintela IA, De Los Reyes BG, Lin CS, Wu VCH. Simultaneous colorimetric detection of a variety of Salmonella spp. In food and environmental samples by optical biosensing using oligonucleotide-gold nanoparticles. Front Microbiol. 2019;10:1–12.
18. Yuan Z, Hu CC, Chang H-T, Lu C. Gold nanoparticles as sensitive optical probes. Analyst. 2016;141(5):1611–26.
19. Gatoo MA, Naseem S, Arfat MY, Mahmood Dar A, Qasim K, Blair S. Physicochemical properties of nanomaterials: Implication in associated toxic manifestations. Biomed Res Int. 2014:1–8.
20. Das M, Shim KH, An SSA, Yi DK. Review on gold nanoparticles and their applications. Toxicol Environ Health Sci. 2011;3(4):193–205.
21. Zhou W, Hu K, Kwee S, Tang L, Wang Z, Xia J, et al. Gold nanoparticle aggregation induced quantitative photothermal biosensing using a thermometer: a simple and universal biosensing platform. Anal Chem. 2020;92(3):2739–47.
22. Annadhasan M, Muthukumarasamyvel T, Sankar Babu VR, Rajendiran N. Green synthesized silver and gold nanoparticles for colorimetric detection of Hg^{2+}, Pb^{2+}, and Mn^{2+} in an aqueous medium. ACS Sustain Chem Eng. 2014;2(4):887–96.
23. Elahi N, Kamali M, Baghersad MH. Recent biomedical applications of gold nanoparticles: A review. Talanta. 2018;184:537–56.
24. Amendola V, Pilot R, Frasconi M, Marago OM, Iati MA. Surface plasmon resonance in gold nanoparticles: A review. J Phys Condens Matter. 2017;29(20):48.
25. Sengani M, Grumezescu AM, Rajeswari VD. Recent trends and methodologies in gold nanoparticle synthesis – A prospective review on drug delivery aspect. OpenNano. 2017;2:37–46.
26. Saha K, Agasti SS, Kim C, Li X, Rotello VM. Gold nanoparticles in chemical and biological sensing. Chem Rev. 2012;112(5):2739–79.
27. Mayer KM, Hafner JH. Localized surface plasmon resonance sensors. Chem Rev. 2011;111(6):3828–57.
28. Chansuvarn W, Tuntulani T, Imyim A. Colorimetric detection of mercury(II) based on gold nanoparticles, fluorescent gold nanoclusters, and other gold-based nanomaterials. TrAC - Trends Anal Chem. 2015;65:83–96.
29. Stewart ME, Anderton CR, Thompson LB, Maria J, Gray SK, Rogers JA, et al. Nanostructured plasmonic sensors. Chem Rev. 2008;108(2):494–521.
30. Vilela D, Gonzalez MC, Escarpa A. Sensing colorimetric approaches based on gold and silver nanoparticles aggregation: Chemical creativity behind the assay. A review. Anal Chim Acta. 2012;751:24–43.
31. Liu G, Lu M, Huang X, Li T, Xu D. Application of gold-nanoparticle colorimetric sensing to rapid food safety screening. Sensors. 2018;18(12):1–16.
32. Li M, Gou H, Al-Ogaidi I, Wu N. Nanostructured sensors for detection of heavy metals: A review. ACS Sustain Chem Eng. 2013;1(7):713–23.
33. Guo L, Xu Y, Ferhan AR, Chen G, Kim DH. Oriented gold nanoparticle aggregation for colorimetric sensors with surprisingly high analytical figures of merit. J Am Chem Soc. 2013;135(33):12338–45.
34. Wang RE, Zhang Y, Cai J, Cai W, Gao T. Aptamer-based fluorescent biosensors. Curr Med Chem. 2011;18(27):4175–84.
35. Wu J, Wang X, Wang Q, Lou Z, Li S, Zhu Y, et al. Nanomaterials with enzyme-like characteristics (nanozymes): Next-generation artificial enzymes (II). Chem Soc Rev. 2019;48(4):1004–76.
36. Zhang X, Wu D, Zhou X, Yu Y, Liu J, Hu N, Wang H, Li G, Wu Y. Recent progress in the construction of nanozyme-based biosensors and their applications to food safety assay. TrAC - Trends Anal Chem. 2019;121:115668.
37. Danzhu Zhu BL, GW. Two-dimensional material-based colorimetric biosensors: a review. Biosensors. 2021;11:259.
38. Lou-Franco J, Das B, Elliott C, Cao C. Gold nanozymes: from concept to biomedical applications. Nano-Micro Letters. 2021;13:1–36.
39. Liu X, Huang D, Lai C, Qin L, Zeng G, Xu P, Li B, Yi H, Zhang M. Peroxidase-like activity of smart nanomaterials and their advanced application in colorimetric. Small. 2019;1900133.
40. Yan Z, Yuan H, Zhao Q, Xing L, Zheng X, Wang W, Zhao Y, Yu Y, Hu L, Yaob W. Recent development of nanoenzyme-based colorimetric sensors for heavy metal detection and the interaction mechanism. Analyst. 2020;145:3173–87.
41. Wang S, Chen W, Liu AL, Hong L, Deng HH, Lin XH. Comparison of the peroxidase-like activity of unmodified, amino-modified, and citrate-capped gold nanoparticles. ChemPhysChem. 2012;13(5):1199–204.

42. Drozd M, Pietrzak M, Parzuchowski PG, Malinowska E. Pitfalls and capabilities of various hydrogen donors in the evaluation of the peroxidase-like activity of gold nanoparticles. Anal Bioanal Chem. 2016;408(29):8505–13.
43. Song W, Zhao B, Wang C, Ozaki Y, Lu X. Functional nanomaterials with unique enzyme-like characteristics for sensing applications. J Mater Chem B. 2019;7(6):850–75.
44. Chatterjee B, Das SJ, Anand A, Sharma TK. Nanozymes and aptamer-based biosensing. Mater Sci Energy Technol. 2020;3:127–35.
45. Sutarlie L, Ow SY, Su X. Nanomaterials-based biosensors for detection of microorganisms and microbial toxins. Biotechnol J. 2017;12(4):1–25.
46. Melikishvili S, Piovarci I, Hianik T. Advances in colorimetric assay based on AuNPs modified by proteins and nucleic acid aptamers. Chemosensors. 2021;9:281.
47. Taghdisi SM, Danesh NM, Ramezani M, Emrani AS, Abnous K. Novel colorimetric aptasensor for zearalenone detection based on nontarget-induced aptamer walker, gold nanoparticles, and exonuclease-assisted recycling amplification. ACS Appl Mater Interfaces. 2018;10(15):12504–9.
48. Duan N, Wu S, Dai S, Gu H, Hao L, Ye H, et al. Advances in aptasensors for the detection of food contaminants. Analyst. 2016;141(13):3942–61.
49. Yan SR, Foroughi MM, Safaei M, Jahani S, Ebrahimpoor N, Borhani F, et al. A Review: Recent advances in ultrasensitive and highly specific recognition aptasensors with various detection strategies. Int J Biol Macromol. 2020;155:184–207.
50. Debiais M, Lelievre A, Smietana M, Müller S. Splitting aptamers and nucleic acid enzymes for the development of advanced biosensors. Nucleic Acids Res. 2020;25:1–23.
51. Seok KY, Ahmad Raston NH, Bock GM. Aptamer-based nanobiosensors. Biosens Bioelectron. 2016;76:2–19.
52. Iliuk AB, Hu L, Tao WA. Aptamer in bioanalytical applications. Anal Chem. 2011:4440–52.
53. Priyadarshini E, Pradhan N. Metal-induced aggregation of valine capped gold nanoparticles: An efficient and rapid approach for colorimetric detection of Pb^{2+} ions. Sci Rep. 2017;7(1):1–8.
54. Shima A, Maryam P, Reza R, Maryam T, Abbas B. Therapeutic applications of nucleic acid aptamers in microbial infections. J Biomed Sci. 2020;27:6.
55. Vivekananda J, Salgado C, Millenbaugh NJ. DNA aptamers as a novel approach to neutralize Staphylococcus aureus α-toxin. Biochem Biophys Res Commun. 2014;444:433–8.
56. Wang K, Gan L, Jiang L, Zhang X, Yang X, Chen M, et al. Neutralization of staphylococcal enterotoxin B by aptamer antagonist. Antimicrob Agents Chemother. 2015;59(4):2072–7.
57. Wang K, Wu D, Chen Z, Zhang X, Yang X, Yang CJ, et al. Inhibition of the superantigenic activities of staphylococcal enterotoxin a by an aptamer antagonist. Toxicon. 2016;119:21–7.
58. Lahousse M, Park H-C, Lee S-C, Ha N-R, Jung I-P, Schlesinger SR, et al. Inhibition of anthrax lethal factor by ssDNA aptamers. Arch Biochem Biophys. 2018;646:16–23.
59. Chang TW, Blank M, Janardhanan P, Singh BR, Mello C, Blind M, et al. In vitro selection of RNA aptamers that inhibit the activity of type a botulinum neurotoxin. Biochem Biophys Res Commun. 2010;396:854–60.
60. Srinivasa M, Ronald RM. Aptamers (Chemical Antibodies) for the mitigation of mycotoxins in domestic livestock. Dairy and Vet Sci J. 2018;7:555714.
61. Sapsford KE, Granek J, Deschamps JR, Boeneman K, Blanco-Canosa JB, Dawson PE, et al. Monitoring botulinum neurotoxin an activity with peptide-functionalized quantum dot resonance energy transfer sensors. ACS Nano. 2011;5(4):2687–99.
62. Dickerson PC, Dickerson TJ. Sensing the deadliest toxin: technologies for botulinum neurotoxin detection. Toxins. 2010;2:24–53.
63. Pirazzini M, Rossetto O, Eleopra R, Montecucco C. Botulinum neurotoxins: Biology, pharmacology, and toxicology. Pharmacol Rev. 2017;69(2):200–35.
64. Janardhanan P, Mello CM, Singh BR, Lou J, Marks JD, Cai S. RNA aptasensor for rapid detection of natively folded type A botulinum neurotoxin. Talanta. 2013;117:273–80.
65. Rosen O, Feldberg L, Gura S, Brosh-Nissimov T, Guri A, Zimhony O, et al. Early, real-time medical diagnosis of botulism by endopeptidase-mass spectrometry. Clin Infect Dis. 2015;61(12):58–61.
66. Wang Y, Fry HC, Skinner GE, Schill KM, Duncan TV. Detection and quantification of biologically active botulinum neurotoxin serotypes A and B using a förster resonance energy transfer-based quantum dot nanobiosensor. ACS Appl Mater Interfaces. 2017;9(37):31446–57.
67. Chen S, Chu LT, Chen TH. Colorimetric detection of active botulinum neurotoxin using Cu2+ mediated gold nanoparticles agglomeration. Sensors Actuators B Chem. 2016;235:563–7.
68. Robert J, Carol A, Christopher D. Rapid detection of botulinum neurotoxins — a review. Toxins. 2019;11:418.
69. Halliwell J, Gwenin C. A label-free colorimetric assay for the detection of active botulinum neurotoxin type a by SNAP-25 conjugated colloidal gold. Toxins. 2013;5(8):1381–91.
70. Chapin KC, Dickenson RA, Wu F, Andrea SB. Comparison of five assays for detection of Clostridium difficile toxin. J Mol Diagnostics. 2011;13(4):395–400.
71. Di Bella S, Ascenzi P, Siarakas S, Petrosillo N, Di Masi A. Clostridium difficile toxins A and B: Insights into pathogenic properties and extraintestinal effects. Toxins. 2016;8(5):1–25.
72. Luo P, Liu Y, Xia Y, Xu H, Xie G. Aptamer biosensor for sensitive detection of toxin A of Clostridium difficile using gold nanoparticles synthesized by Bacillus stearothermophilus. Biosens Bioelectron. 2014;54:217–21.
73. Al-Saadi T, Eltai N, Hamdi W, Bakhsh F, Azazzy H, Al-Ansari N, et al. Colorimetric gold nanoparticles-based assay for direct detection of Clostridium difficile in clinical isolates from Qatar. African J Microbiol Res. 2017;11(19):756–63.
74. Yang M, Kostov Y, Bruck HA, Rasooly A. Gold nanoparticle-based enhanced chemiluminescence immunosensor for detection of Staphylococcal Enterotoxin B (SEB) in food. Int J Food Microbiol. 2009;133(3):265–71.
75. Zhu S, Du CL, Fu Y. Localized surface plasmon resonance-based hybrid Au-Ag nanoparticles for detection of Staphylococcus aureus enterotoxin B. Opt Mater (Amst). 2009;31(11):1608–13.
76. Xu Y, Huo B, Sun X, Ning B, Peng Y, Bai J, et al. Rapid detection of staphylococcal enterotoxin B in milk samples based on fluorescence hybridization chain reaction amplification. RSC Adv. 2018;8(29):16024–31.
77. Sapsford KE, Taitt CR, Loo N, Ligler FS. Biosensor detection of botulinum toxoid a and staphylococcal enterotoxin B in food. Appl Environ Microbiol. 2005;71(9):5590–2.
78. Mondal B, Ramlal S, Lavu PS, Bhavanashri N, Kingston J. Highly sensitive colorimetric biosensor for staphylococcal enterotoxin B by a label-free aptamer and gold nanoparticles. Front Microbiol. 2018;9:1–8.
79. Liu A, Zhang Y, Chen W, Wang X, Chen F. Gold nanoparticle-based colorimetric detection of staphylococcal enterotoxin B using ssDNA aptamers. Eur Food Res Technol. 2013;237(3):323–9.
80. Zhou D, Xie G, Cao X, Chen X, Zhang X, Chen H. Colorimetric determination of staphylococcal enterotoxin B via DNAzyme-guided growth of gold nanoparticles. Microchim Acta. 2016;183(10):2753–60.

81. Shkembi X, Svobodova M, Skouridou V, Bashammakh AS, Alyoubi AO, O'Sullivan CK. Aptasensors for mycotoxin detection: A review. Anal Biochem. 2022;644:114156.
82. Marchese S, Polo A, Ariano A, Velotto S, Costantini S, Severino L. Aflatoxin B1 and M1: Biological properties and their involvement in cancer development. Toxins. 2018;10(6):1–19.
83. Wu J, Zeng L, Li N, Liu C, Chen J. A wash-free and label-free colorimetric biosensor for naked-eye detection of aflatoxin B1 using G-quadruplex as the signal reporter. Food Chem. 2019;298:125034.
84. Li X, Yang F, Wong JXH, Yu HZ. Integrated smartphone-app-chip system for on-site parts-per-billion-level colorimetric quantitation of aflatoxins. Anal Chem. 2017;89(17):8908–16.
85. Jia Y, Zhou G, Liu P, Li Z, Yu B. Recent development of aptamer sensors for the quantification of aflatoxin B1. Appl Sci. 2019;9(11):1–17.
86. Man Y, Liang G, Li A, Pan L. Recent advances in mycotoxin determination for food monitoring via microchip. Toxins. 2017;9:324.
87. Danesh NM, Bostan HB, Abnous K, Ramezani M, Youssefi K, Taghdisi SM, et al. Ultrasensitive detection of aflatoxin B1 and its major metabolite aflatoxin M1 using aptasensors: A review. TrAC - Trends Anal Chem. 2018;99:117–28.
88. Guo X, Wen F, Zheng N, Luo Q, Wang H, Wang H, et al. Development of an ultrasensitive aptasensor for the detection of aflatoxin B1. Biosens Bioelectron. 2014;56:340–4.
89. Wang Q, Yang Q, Wu W. Progress on structured biosensors for monitoring aflatoxin b1 from biofilms: a review. Front Microbiol. 2020;11:1–15.
90. Ferreira IMPLVO, Mendes E, Oliveira MBPP. Quantification of Aflatoxins B1, B2, G1, and G2 in Pepper by HPLC/Fluorescence. J Liq Chromatogr Relat Technol. 2004;27(2):325–34.
91. Li Y, Wen S, Chen Z, Xiao Z, Ma M. Ultra-high performance liquid chromatography-tandem mass spectrometry for simultaneous analysis of aflatoxins B1, G1, B2, G2, zearalenone and its metabolites in eggs using a QuEChERS-based extraction procedure. Anal Methods. 2015;7(10):4145–51.
92. Wei R, Qiu F, Kong W, Wei J, Yang M, Luo Z, et al. Co-occurrence of aflatoxin B1, B2, G1, G2 and ochratoxin A in Glycyrrhiza uralensis analyzed by HPLC-MS/MS. Food Control. 2013;32(1):216–21.
93. Ren M, Xu H, Huang X, Kuang M, Xiong Y, Xu H, et al. Immunochromatographic assay for ultrasensitive detection of aflatoxin B1 in maize by highly luminescent quantum dot beads. ACS Appl Mater Interfaces. 2014;6(16):14215–22.
94. Anfossi L, Baggiani C, Giovannoli C, Giraudi G. Lateral flow immunoassays for aflatoxins B and G and aflatoxin M1. In: Razzaghi-Abyaneh, M. , editor. Aflatoxins - recent Adv futur prospect. 2013; London: IntechOpen; 2013 [cited 2022 Jun 11]. Available from: https://www.intechopen.com/chapters/40108, https://doi.org/10.5772/51777.
95. Li P, Zhou Q, Wang T, Zhou H, Zhang W, Ding X, et al. Development of an enzyme-linked immunosorbent assay method specific for the detection of G-group aflatoxins. Toxins. 2015;8(1):1–11.
96. Paniel N, Radoi A, Marty JL. Development of an electrochemical biosensor for the detection of aflatoxin M1 in Milk. Sensors. 2010;10(10):9439–48.
97. Kasoju A, Shrikrishna NS, Shahdeo D, Khan AA, Alanazi AM, Gandhi S. Microfluidic paper device for rapid detection of aflatoxin B1 using an aptamer-based colorimetric assay. RSC Adv. 2020;10(20):11843–50.
98. Kasoju A, Shahdeo D, Khan AA, Shrikrishna NS, Mahari S, Alanazi AM, et al. Fabrication of microfluidic device for Aflatoxin M1 detection in milk samples with specific aptamers. Sci Rep. 2020;10(1):1–8.
99. Luan Y, Chen Z, Xie G, Chen J, Lu A, Li C, et al. Rapid visual detection of aflatoxin B1 by label-free aptasensor using unmodified gold nanoparticles. J Nanosci Nanotechnol. 2015;15(2):1357–61.
100. Chen J, Wen J, Zhuang L, Zhou S. An enzyme-free catalytic DNA circuit for amplified detection of aflatoxin B1 using gold nanoparticles as colorimetric indicators. Nanoscale. 2016;8(18):9791–7.
101. Zhu W, Li L, Zhou Z, Yang X, Hao N, Guo Y, et al. A colorimetric biosensor for simultaneous ochratoxin A and aflatoxins B1 detection in agricultural products. Food Chem. 2020;319:126544.
102. Lerdsri J, Chananchana W, Upan J, Sridara T, Jakmunee J. Label-free colorimetric aptasensor for rapid detection of aflatoxin B1 by utilizing cationic perylene probe and localized surface plasmon resonance of gold nanoparticles. Sensors Actuators, B Chem. 2020;320:128356.
103. Luan Y, Chen J, Xie G, Li C, Ping H, Ma Z, et al. Visual and microplate detection of aflatoxin B2 based on NaCl-induced aggregation of aptamer-modified gold nanoparticles. Microchim Acta. 2015;182(5–6):995–1001.
104. Lerdsri J, Soongsong J, Laolue P, Jakmunee J. Reliable colorimetric aptasensor exploiting 72-Mers ssDNA and gold nanoprobes for highly sensitive detection of aflatoxin M1 in milk. J Food Compos Anal. 2021;102:103992.
105. Jalalian SH, Lavaee P, Ramezani M, Taghdisi SM. An optical aptasensor for aflatoxin M1 detection based on target-induced protection of gold nanoparticles against salt-induced aggregation and silica nanoparticles. Spectrochim Acta Part A Mol Biomol Spectrosc. 2020;119062.
106. Abnous K, Mohammad N, Ramezani M, Alibolandi M, Alin ezhad M, Sadat T, et al. A novel colorimetric aptasensor for ultrasensitive detection of aflatoxin M1 based on the combination of CRISPR-Cas12a, rolling circle amplification and catalytic activity of gold nanoparticles. Anal Chim Acta. 2021;1165:338549.
107. Gil-Serna J, Vazquez C, Gonzalez-Jaen M, Patino B. Wine Contamination with Ochratoxins: A Review. Beverages. 2018;4(1):6.
108. Lv L, Li D, Liu R, Cui C, Guo Z. Label-free aptasensor for ochratoxin A detection using SYBR Gold as a probe. Sensors Actuators, B Chem. 2017;246:647–52.
109. Pagkali V, Petrou PS, Salapatas A, Makarona E, Peters J, Haasnoot W, et al. Detection of ochratoxin A in beer samples with a label-free monolithically integrated optoelectronic biosensor. J Hazard Mater. 2017;323:75–83.
110. Yu X, Lin Y, Wang X, Xu L, Wang Z, Fu FF. Exonuclease-assisted multicolor aptasensor for visual detection of ochratoxin A based on G-quadruplex-hemin DNAzyme-mediated etching of gold nanorod. Microchim Acta. 2018;185(5):1–9.
111. Tian F, Zhou J, Fu R, Cui Y, Zhao Q, Jiao B, et al. Multicolor colorimetric detection of ochratoxin A via structure-switching aptamer and enzyme-induced metallization of gold nanorods. Food Chem. 2020;320:126607.
112. Ha TH. Recent Advances for the Detection of Ochratoxin A. Toxins. 2015;7:5276–300.
113. Lee J, Jeon CH, Ahn SJ, Ha TH. Highly stable colorimetric aptamer sensors for detection of ochratoxin A through optimizing the sequence with the covalent conjugation of hemin. Analyst. 2014;139(7):1622–7.
114. Damiano S, Andretta E, Longobardi C, Prisco F, Paciello O, Squillacioti C, et al. Effects of curcumin on the renal toxicity induced by ochratoxin A in rats. Antioxidants. 2020;9:332.
115. Liu B, Huang R, Yu Y, Su R, Qi W, He Z. Gold nanoparticle-aptamer-based LSPR sensing of ochratoxin A at a widened detection range by double calibration curve method. Front. Chem. 2018;6:94.

116. Lee B, Park JH, Byun JY, Kim JH, Kim MG. An optical fiber-based LSPR aptasensor for simple and rapid in-situ detection of ochratoxin A. Biosens Bioelectron. 2018;102:504–9.
117. Duarte SC, Pena A, Lino CM. A review on ochratoxin A occurrence and effects of processing of cereal and cereal-derived food products. Food Microbiol. 2010;27(2):187–98.
118. Tian F, Zhou J, Jiao B, He Y. A nanozyme-based cascade colorimetric aptasensor for amplified detection of ochratoxin A. Nanoscale. 2019;11(19):9547–55.
119. Luan Y, Chen J, Li C, Xie G, Fu H, Ma Z. Highly sensitive colorimetric detection of ochratoxin A by a label-free aptamer and gold nanoparticles. Toxins. 2015:5377–85.
120. Xiao R, Wang D, Lin Z, Qiu B, Liu M, Guo L, Chen G. Disassembly of gold nanoparticle dimers for colorimetric detection of ochratoxin A. Anal Methods. 2015;7(3):842–5.
121. Yang C, Wang Y, Marty JL, Yang X. Aptamer-based colorimetric biosensing of Ochratoxin A using unmodified gold nanoparticles indicator. Biosens Bioelectron. 2011;26(5):2724–7.
122. Tian F, Zhou J, Fu R, Cui Y, Zhao Q, Jiao B, Yue H. Multicolor colorimetric detection of ochratoxin A via structure-switching aptamer and enzyme-induced metallization of gold nanorods. Food Chem. 2020;320:126607.
123. Wang C, Qian J, Wang K, Yang X, Liu Q, Hao N, Guo Y, Wang K. Colorimetric aptasensing of ochratoxin A using Au@Fe_3O_4 nanoparticles as the signal indicator and magnetic separator. Biosens Bioelectron. 2016;77:1183–91.
124. Liu R, Huang Y, Ma Y, Jia S, Gao M, Li J, Zhang H, Xu D, Wu M, Chen Y, Zhu Z, Yang C. Design and synthesis of target-responsive aptamer-cross-linked hydrogel for visual quantitative detection of ochratoxin A. ACS Appl Mater Interfaces. 2015;7(12):6982–90.
125. Caglayan MO, Ustundag Z. Detection of zearalenone in an aptamer assay using attenuated internal reflection ellipsometry and its cereal sample applications. Food Chem Toxicol. 2020;136:111081.
126. Sun S, Zhao R, Feng S, Xie Y. Colorimetric zearalenone assay based on the use of an aptamer and of gold nanoparticles with peroxidase-like activity. Microchim Acta. 2018;185(12):1–7.
127. Liu M, Zhao H, Chen S, Yu H, Quan X. Colloidal graphene as a transducer in homogeneous fluorescence-based immune-sensor for rapid and sensitive analysis of microcystin-LR. Environ Sci Technol. 2012;46(22):12567–74.
128. Wu S, Duan N, Zhang H, Wang Z. Simultaneous detection of microcystin-LR and okadaic acid using a dual fluorescence resonance energy transfer aptasensor. Anal Bioanal Chem. 2015;407(5):1303–12.
129. Eissa S, Ng A, Siaj M, Zourob M. Label-free voltammetric aptasensor for the sensitive detection of microcystin-LR using graphene-modified electrodes. Anal Chem. 2014;86(15):7551–7.
130. Chen K, Liu M, Zhao G, Shi H, Fan L, Zhao S. Fabrication of a novel and simple microcystin-LR photoelectrochemical sensor with high sensitivity and selectivity. Environ Sci Technol. 2012;46(21):11955–61.
131. Bostan HB, Taghdisi SM, Bowen JL, Demertzis N, Rezaee R, Panahi Y, Tsatsakise AM, Karimif G. Determination of microcystin-LR, employing aptasensors. Biosens Bioelectron. 2018;119:110–8.
132. Epa US. Drinking-water health advisory for the cyanobacterial microcystin toxins. https://www.epa.gov/sites/default/files/2017-06/documents/microcystins-report-2015.pdf.
133. Neumann AC, Wang X, Niessner R, Knopp D. Determination of microcystin-LR in surface water by a magnetic bead-based colorimetric immunoassay using antibody-conjugated gold nanoparticles. Anal Methods. 2016;8(1):57–63.
134. Tang X, Yin Z, Lei X, Wu X, Zeng Y, Zhang Z, Lu Y. Colorimetric method for sensitive detection of microcystin-LR using surface copper nanoparticles of polydopamine nanosphere as turn-on probe. Nanomaterials. 2019;9(3):332.
135. Bickman SR, Campbell K, Elliott C, Murphy C, O'Kennedy R, Papst P, Lochhead M. An innovative portable biosensor system for the rapid detection of freshwater cyanobacterial algal bloom toxins. Environ Sci Technol. 2018;52(20):11691–8.
136. Zhu Y, Xu L, Ma W, Chen W, Yan W, Kuang H, Wang L, Xua C. G-quadruplex DNAzyme-based microcystin-LR (toxin) determination by a novel immunosensor. Biosens Bioelectron. 2011;26(11):4393–8.
137. Lv J, Zhao S, Wu S, Wang Z. Upconversion nanoparticles grafted molybdenum disulfide nanosheets platform for microcystin-LR sensing. Biosens Bioelectron. 2017;90:203–9.
138. Li X, Cheng R, Shi H, Tang B, Xiao H, Zhao G. A simple highly sensitive, and selective aptamer-based colorimetric sensor for environmental toxins microcystin-LR in water samples. J Hazard Mater. 2016;304:474–80.
139. Wang F, Liu S, Lin M, Chen X, Lin S, Du X, et al. Colorimetric detection of microcystin-LR based on disassembly of orient-aggregated gold nanoparticle dimers. Biosens Bioelectron. 2015;68:475–80.
140. Feng J, Wu Y, Shen Q. A simple and selective colorimetric aptasensor for detection of toxins microcystin-lr in fish tissue using a truncated aptamer. Food Anal Methods. 2022; Available from: https://doi.org/10.1007/s12161-022-02283-6.
141. Ye W, Liu T, Zhang W, Zhu M, Liu Z, Kong Y, Liu S. Marine toxins detection by biosensors based on aptamers. Toxins. 2019;12(1):1–22.
142. Qiang L, Zhang Y, Guo X, Gao Y, Han Y, Sun J. A rapid and ultrasensitive colorimetric biosensor based on aptamer functionalized Au nanoparticles for detection of saxitoxin. RSC Adv. 2020;2020:15293–8.
143. Zhao Y, Li L, Ma R, Wang L, Yan X, Qi X, Wang S, MaoX. A competitive colorimetric aptasensor transduced by hybridization chain reaction-facilitated catalysis of AuNPs nanozyme for highly sensitive detection of saxitoxin. Anal Chim Acta. 2021;1173:338710.